Characterisation of a Parabolic Trough Collector Using Sheet Metal and Glass Mirror Strips

by

O. R. Woodrow

A dissertation in partial fulfilment of the requirements for the degree Master of Engineering in Chemical Engineering

Department of Chemical Engineering

Faculty of Engineering, Built Environment and IT

University of Pretoria

South Africa

December 2016

Supervisor: Dr. Heinrich Badenhorst

CVD 800

Declaration

I, Oliver Rhys Woodrow, hereby declare that this Master's dissertation is my own original work. I have not copied from any other student's work or from any other sources except where due reference or acknowledgement is made explicitly in the text, nor has any part been written for me by another person.

It is the intention that this Masters dissertation be submitted for the degree of Master of Engineering in Chemical Engineering at the University of Pretoria. Therefore I further declare that this dissertation has not been submitted to any other educational institution for any examination, diploma, degree or other form of qualification.

_____ December 2016

Oliver Rhys Woodrow

Synopsis

A novel type of parabolic trough collector was characterised using a very basic theoretical model. This model looked at an ideal case and provided a basic expectation that was compared to actual measurements. The model showed that greater improvements can be achieved if heat losses to the environment are limited or omitted. This can be achieved by using a glass shield to insulate the receiver in a vacuum to limit the effect wind has and therefore limit convective losses.

The experimental characterisation of the PTC consisted of taking six different temperature measurements to better understand the energy balances taking place. Four different configurations were tested, using two different types of concentrator and in each case a receiver that was either unpainted or painted with a semi matte black paint. The different types of concentrator were either stainless steel sheet metal or discretised glass mirror strips, similar to a linear Fresnel collector. Experimental runs were conducted on cloudless days for an hour and 15 minutes. This allowed for three runs to be performed on a single day. Using the theoretical model and comparing it to the experimental data, an efficiency was calculated. This efficiency averaged 14 % when the receiver was unpainted and 13 % when the receiver was painted for the metal sheets. The glass mirror strips had average efficiencies of 54 % and 45 % for an unpainted and painted receiver respectively. The model is very basic and can be improved upon if more variables are taken into consideration, such as convective heat losses. It was also recommended that wind measurements are taken in future tests.

A property looked at to evaluate the effectiveness of each type of configuration was the average energy supplied to the thermal heating fluid over the course of an experimental run. For this the averaged values over all the experimental runs conducted for stainless steel sheet metal were 258 W and 332 W for an unpainted and painted pipe respectively. When using the glass mirrors an average energy value of 1049 W was supplied when the pipe was unpainted and an average of 1181 W was gained in the runs conducted after the pipe had been painted.

Painting the receiver had little to no effect. The surface temperature of the receiver after painting the pipe was not higher and a slight increase in the energy gained by water was observed. This was explained by inaccuracies during testing as scattered light may have caused an interference on some of the measurements. There were also human inaccuracies in testing which should be omitted in future tests by implementing, for one, a functional tracking system. Future tests should be designed in such a way to completely omit irradiance affecting the thermocouple taking the measurement.

Glass mirrors fared far better than the stainless steel sheet metal counterpart. It was recommended that they are used as the concentrator of choice. Higher efficiencies were achieved and in some cases almost four times the energy was supplied to the water in the

pipe. This was attributed to a much lower concentrator temperature, on average 11 °C lower than the temperature of the metal sheets, as well as a much better ability to concentrate sunlight onto a single focal point. However, the glass mirror strips were proven to be very fragile and as such, require protection from the elements. While the strips were lighter and caused less of a load during windy conditions, they were susceptible to oscillations from gusty wind. This led to a number of strips breaking and needed to be replaced. By discretising the strips into individual pieces, they had the benefit of only needing to replace the strips that were damaged. This is also true for all future runs. It is still recommended that a tarp be used to protect the glass mirrors.

Using glass mirror strips as a concentrator combined LFC technology with PTC technology and a novel PTC design was achieved. The design still required the installation area of a PTC. The novel design was compared to Industrial Solar's industrial LFC module, LF-11, as it shares many similarities to LFC technology. The peak thermal output of the rig was significantly lower at 346 W/m^2 compared to the industrial value of 562 W/m^2. However, the noteworthy differences in design and optimisation between the two modules meant the results achieved were comparable. It is expected that better and more comparable results can be realised once the inherent flaws in the design, such as tracking the sun, aperture size and adding a vacuum absorber, are addressed. It is recommended that more research and emphasis is put into this field as an alternative energy power plant for South Africa.

Keywords: **concentrated solar power, parabolic trough collector, linear Fresnel collector**

Acknowledgements

Firstly, I would like to thank the National Research Fund (NRF) for their funding of this research. I would also like to thank them for supporting me financially through this master's research. Secondly, to my supervisor, Heinrich Badenhorst, thank you for suggesting such a fun and different topic that has challenged me and kept me interested. Thank you so much for your guidance, your patience and your understanding. Lastly, thank you to all my friends and family for your continuous interest and questioning. Thank you for encouraging me when I was down and praising me when I got results. Especially thank you Mom, for kicking me when I needed it, thank you Dad for your help and editing and last but most of all thank you Lucja. Without your persistence and your immeasurable help I would likely not have finished. I cannot express in words how grateful I am.

For Emma.

Contents

List of Figures

List of Tables

List of Abbreviations

Avg	Average
CSP	Concentrated solar power
DNI	Direct normal irradiance
DHI	Diffused horizontal irradiance
GHI	Global horizontal irradiance
ID	Internal diameter
LFC	Linear Fresnel Collector
P & ID	Piping and instrumentation diagram
PTC	Parabolic trough collector
PVC	Polyvinyl chloride
SAURAN	South African Universities Radiometric Network
Std Dev	Standard Deviation
THF	Thermal heating fluid

Nomenclature

Roman symbols

c_p	Heat capacity	J/kg.K
D	Internal diameter	m
h	Convective heat transfer coefficient	W/m^2K
İ	Irradiance	W/m^2
$\dot{m}$	Rate of mass transfer	kg/s
$\dot{Q}$	Rate of energy transfer	W
Re	Reynolds number	
T	Temperature	°C
v	Linear velocity	m/s

Greek symbols

α	Absorptivity of the material	
Δ	Difference	
ε	Emissivity of the material	
η	Efficiency	%
θ	Angle the sun makes with the earth's surface	°
μ	Viscosity of the medium	Pa.s
ρ	Density of the medium	kg/m^3
σ	Stefan Boltzmann constant	$W/m^2.K^4$

Subscripts

actual	Actual
e	Exit
env	Environment
conc	Concentrator
conv	Convection
i	Inlet
losses	Losses
rad	Radiaton
rec	Receiver
s	Surface of the receiver
solar,incident	Solar incident from the sun
surr	Surroundings
theo	Theoretical

Chapter 1: Introduction

1.1 Background

In the late twentieth century scientists agreed that the average global temperature was rising. This was attributed to pollutants, the so-called greenhouse gases, which prohibit the sun's radiation waves from exiting the earth's atmosphere. This phenomenon in turn causes the earth's temperature to rise and was aptly named global warming. While postulated theories have varied widely about melting icecaps, rising sea levels and global scale catastrophe, one common recommendation has been prevalent: the mitigation of the emission of greenhouse gases. Rules and regulations have been put into place in order to limit the amount of greenhouse gases produced and fed into the atmosphere, such as South Africa's Air Quality Act (39/2004) (Government Gazette (2010)). Alternative solutions have been (and still are being) researched to find ways and means of achieving the same electricity production without causing pollution.

One of the chief contributors of greenhouse gas emissions is coal power plants. This poses a significant problem, because global energy demands increase as the human population does. Alternative energy solutions exist, such as nuclear energy, but this has its own set of problems and pollution. As such, there is a global drive to research and implement renewable energy solutions, such as hydro, wind, biomass or solar energy.

1.2 Objective

The objective of this study is to characterise, as well as test the viability of, a novel design of a parabolic trough collector (PTC). The aim is firstly to set up a basic theoretical model for the PTC. Secondly a greater understanding of the PTC is required which is achieved by taking various temperature measurements from which the energy transferred to the thermal heating fluid can be calculated. Thirdly the theoretical model is compared with actual results. Finally a comparison of the novel PTC is made to an industrial Linear Fresnel Collector (LFC).

The hypothesis is that combining PTC and LFC technologies and using singular glass mirror strips as a concentrator will yield comparable results to what is currently being researched and implemented at industry level. Mirror strips have significant advantages over a single, large, curved mirror, such as, lower manufacturing cost, less wind resistance and they can be individually replaced if necessary. For comparative purposes, tests using sheets of stainless steel were also carried out. This document serves to comment on the findings and recommendations of these concentrated solar power (CSP) tests.

1.3 Method

In order to characterise and compare different concentrators for a parabolic trough collector, water is pumped through the system. The concentrators used are stainless steel metal sheets and discretised mirror strips. Six thermocouples measure the following: the inlet and outlet temperature of the heating fluid, water; the surface temperature of the pipe being heated; the temperature of the concentrator; the temperature of the water reservoir and the ambient temperature. Tests are done on cloudless days to try and ensure conditions are mostly kept constant. The collected data is analysed and compared and the main findings are then reported.

1.4 Application of Research

South Africa may be well suited to the application of concentrated solar power. It has vast areas that receive a high incidence of solar radiation. By characterising and testing a parabolic trough collector, the ground work for potential future implementation is done. For the design to be considered for industrial applications, more research on using multiples PTCs in series will be required. Since the system is designed to be self-sustainable, an alternative application that could be considered is heating up water for rural townships. This water could be used for bathing or washing of clothes.

1.5 Structure of Dissertation

The dissertation is divided into the following chapters:

- **Chapter 2:** research and literary findings pertaining to the field of study are discussed. An emphasis is placed on parabolic trough collectors and a basic model for the setup is designed.
- **Chapter 3:** the experimental setup, as well as the experimental procedure are fully explained. Photographs and drawings of the setup are included for supplementary understanding.
- **Chapter 4:** in this chapter the raw data for the four different configurational setups is reported and the findings of that data discussed.
- **Chapter 5:** focuses on comparing the different configurations, first by changing properties of the receiver, then by changing the type of concentrator.
- **Chapter 6:** in the last chapter all conclusions are stated and recommendations for the future are prescribed.
- **Chapter 7:** lists all references used in alphabetical order.

Chapter 2: Literature Review

2.1 Renewable energy

As the world's population grows so do the ever increasing energy demands. Globalisation has also led to people seeking better living standards, which in turn requires more electricity. According to the World Meteorological Organisation (2016) this has led to the continued increase of greenhouse gases in the atmosphere. A major contributing factor is the pollution caused by burning fossil fuels and ultimately greenhouse gases may lead to a global climate change. As such, alternative, sustainable energy solutions are sought to meet the demand for electricity without producing additional greenhouse gases. Renewable energy has received a lot of attention in recent times, because of its potential to replace fossil fuels (REN21, 2016). Renewable energy is sustainable and does not produce harmful by-products. Examples of renewable energy are wind, hydro, solar energy and biofuels.

According to a report by REN21 (2016) hydro energy constitutes the largest portion of renewable energies, having a total capacity of 1064 GW of a total 1849 GW globally. Unfortunately there is a limit to the energy that can be produced from hydro power plants and alternatives are needed. Some novel methods have been and are being researched to try and exploit the natural motion present in the ocean. Wind energy is arguably at the forefront as an alternative to hydro energy. It has been met with criticism for being aesthetically unpleasing to look at and its consequences are not necessarily all understood. However, if implemented in a windy area it does have many advantages. It can be built atop of hills to maximise the wind a turbine would receive. It can also produce electricity throughout the day and night, which solar energy cannot do. Solar energy is dependent on sunshine and can fail even on overly clouded days. Biofuels is a field that is gaining attention quickly. It has the benefit of using existing technologies and simply replacing the fuel that is currently used. The biggest challenge biofuels face is achieving the same efficiency as fossil fuels.

There are a number of methods in solar energy that suit different applications. Photovoltaics have drawn a lot of attention since they convert solar energy directly into electricity. Solar panels using this technology are quite common and commercially available. They are, however, limited by a poor efficiency (Wilson & Emery, 2014). Because of this, there is a lot of research in coming up with a more efficient solar panel. Higher efficiencies have been achieved (Conibeer, 2007; Wilson & Emery, 2014), but such panels are considerably more expensive. There is a compromise between efficiency and cost and as of yet, an inexpensive solar panel with a high efficiency has not been found. An alternative to photovoltaics is artificial photosynthesis. The natural process of photosynthesis is mimicked and energy is stored into a solar fuel. A common topic of study in this field is the photocatalytic splitting of water. The other method of harnessing the suns energy is solar heating. This is common for swimming pools and geysers, where water is pumped through a high surface area that is exposed to sunlight. Typically this area is black to achieve a high absorbance of the incident sunlight. In

this manner the water is heated for later use. A similar method has also developed into its own field of study by concentrating the sunlight onto a focal point and uses the thermal energy to heat up a thermal heating fluid (THF). This method is called concentrated solar power (CSP).

2.2 Concentrated Solar Power

Different designs exist to concentrate the sun's thermal energy, namely parabolic trough, Sterling dish, Fresnel reflector and solar power tower. A basic drawing of the most common designs found in industry can be seen in Figure 2-1. In each case the concentrators, usually mirrors or a heliostat, focus the sun rays onto a focal point, the receiver. This holds the thermal media or THF, such as oil. The THF is used to transport the energy to a thermal storage, which is usually in the form of a salt or salt mixture. Thermal storage is very important because CSP plants operate most effectively in the middle of the day, but electricity demands are highest in the evening. Thermal storage allows the stored energy to be converted to electricity at a later stage when it is most needed. This is usually achieved using a standard Rankine cycle (Österholm & Pålsson, 2014). Each design has its own advantages and drawbacks. Depending on the design used, a tracking system along either one axis (West – East) or two axes (additionally North – South) is used. A system using a single axis offers a lower cost, but also a lower performance output, when compared to a two axis tracking system.

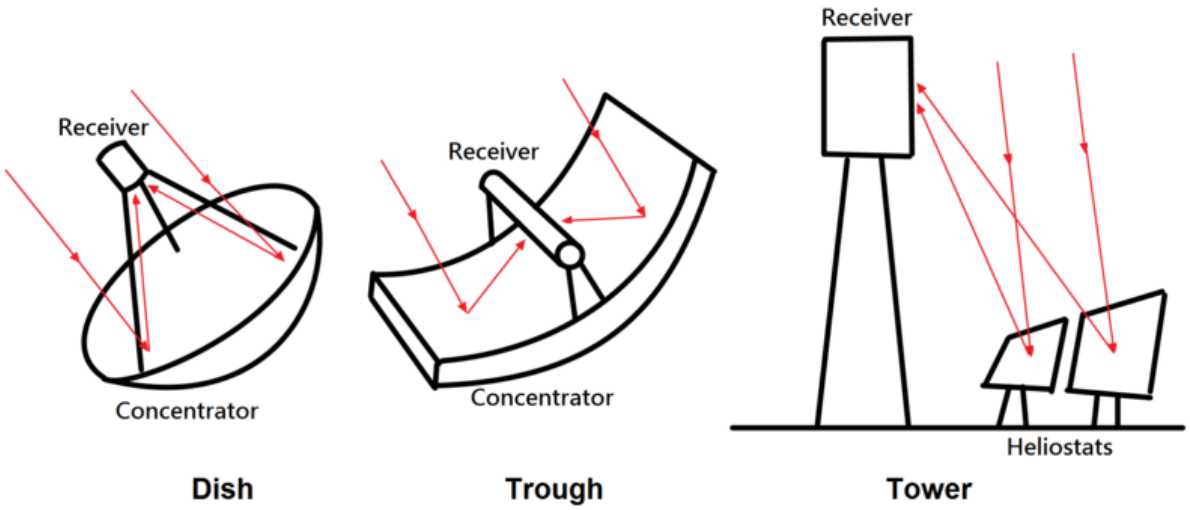

Figure 2-1: Basic representation of the most common concentrated solar power designs found in industry.

In some instances a Fresnel lens may be used in conjunction with CSP plants if it is required to further focus the sunlight onto a single point, however the present application remains small (Xie *et al*, 2011). A Fresnel lens, named after Augustin-Jean Fresnel, is a standard lens projected onto a flat surface. This is achieved by dividing the flat surface into discontinuous sections, each at a different angle, in order to achieve a single focal point. An illustration of a Fresnel lens compared to a standard lens can be seen in Figure 2-2. The standard lens is

seen atop the Fresnel lens. The discontinuities make the Fresnel lens look like a set of concentric rings when viewed from the top.

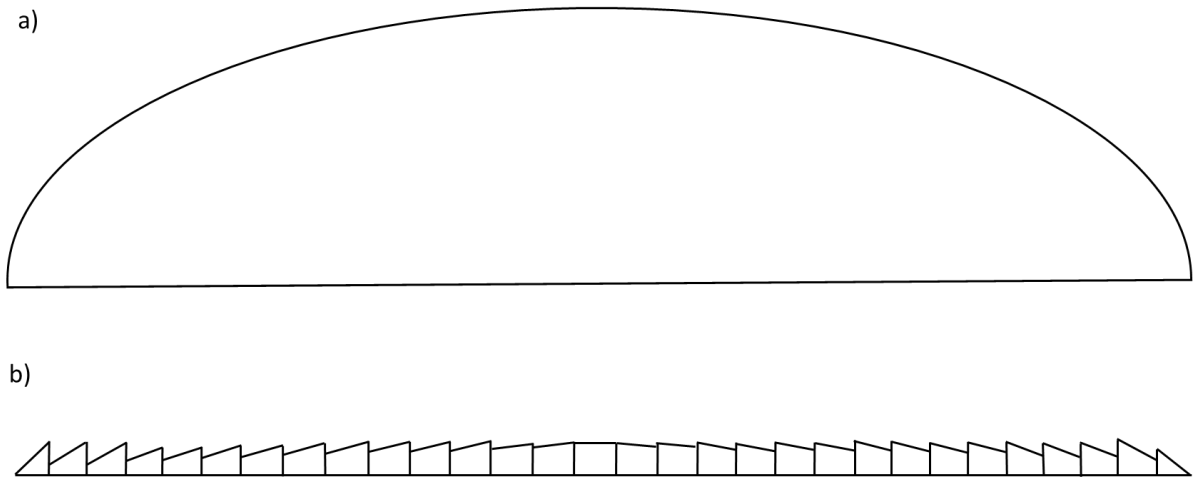

Figure 2-2: A simplified drawing of a standard lens (a) versus a Fresnel lens (b)

A method of implementing Fresnel technology for CSP plants exists in the form of Linear Fresnel Collectors (LFCs). The setup is similar to a parabolic trough collector, however, instead of using a single curved mirror, a series of long flat mirrors is used. These are operated individually so that each strip focuses sunlight onto the fixed receiver overhead. The disadvantage this technology has is the focal line is distorted by astigmatism. It is therefore recommended that a secondary reflector above the receiver is used to capture the distorted rays (IRENA, 2012). Another drawback is the optical efficiency of LFCs is lower than in standard PTC configurations, because of the geometric properties. However, they do also have a number of advantages, such as being less expensive to produce, being lighter and having an easier assembly, as well as significantly reduced wind loads.

CSP plants are best suited to arid regions with little or no cloud cover as this maximises the irradiation from the sun. The leading countries in the industry are the United States of America and Spain. In the US there already exist a number of plants that are being used as an alternative energy source. According to Sawin & Martinot (2011) by the end of 2010 Spain produced 632 MW and USA 509 MW with more plants commissioned. Österholm & Pålsson (2014) refer to one of the largest parabolic trough type plants in operation, the Shams 1, in the United Arab Emirates.

There are other applications of concentrated solar energy apart from producing electricity. One example of this is to use concentrated solar energy in reactor designs, eliminating the need to add heat externally. The field is a fast-growing industry, with massive potential returns, however, a major drawback is the high manufacturing cost of the specialised, curved mirrors. More focus will be given to parabolic trough collectors (PTCs) as they are the most common design found in industry. IRENA (2012) lists that over 90 % of CSP plants operate on PTCs.

The design tested in this research is also a PTC design. South Africa has vast, unpopulated areas that receive a high incidence of sun rays. Therefore it would suit concentrated solar power well and application in South Africa is also considered.

2.3 Parabolic Trough Collectors

A very basic form of a PTC has been illustrated in the previous section. The parabola shape has a single focal point above it, where its height depends on the curvature of the parabola. Typically a pipe will function as the receiver in this setup. As mentioned previously, concentrated solar power is the field where light is concentrated onto a focal point in order to generate heat. This thermal energy is then commonly used to generate electricity such as in a steam cycle. Sawin and Martinot (2011) also claim that PTCs account for 90 % of all power plants, similar to IRENA (2012). For this reason the focus of this literature will be placed on the parabolic trough design.

As the name suggests, a parabolic trough is a channel in the shape of a parabola. The parabola is usually made of a highly reflective material, such as a mirror. This surface reflects incident light beams onto a common focal area, F. This is illustrated in Figure 2-3 below.

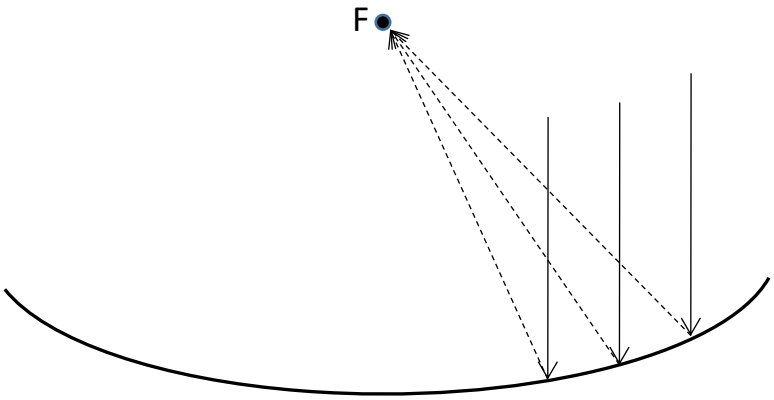

Figure 2-3: Illustration of a parabolic trough reflecting incident beams onto a common focal point

As can be seen from Figure 2-3, the incident beams are required to be parallel to the axis of symmetry of the parabolic trough in order for them to be reflected onto the point F. This illustrates the need for a good tracking system. Most parabolic troughs are aligned North to South and to achieve the desired concentrating effect of light, the parabola must always be perpendicular to the sun's incidence.

One major setback of PTCs is the high manufacturing cost involved in manufacturing smooth, curved mirrors. These can easily have defects which would decrease the efficiency of the

collector. Therefore, care must be in taken in the manufacturing process which drives up the cost. As a result there is a lot of research conducted to try and improve current PTC designs and their respective efficiency. Kumar and Reddy (2012) found in their research that use of a porous disc receiver increased the performance of a solar parabolic trough. They could achieve this, because the porous disc increased the heat transfer rate. However, there was a penalty to the pressure drop and subsequent pumping penalty. Meiser *et al* (2014) show in their work the importance of positioning and mounting for mirror shape accuracy. They also investigated different types of frames, namely a rigid frame, a laboratory support frame and a frame with elastic brackets. Depending on the frame and positioning relevant deviations can be picked up. Another paper by Barriga *et al* (2014) explores the possibility of increasing the performance of a PTC by adding a selective absorber coating. The PTCs are wanted to be operated at 600 °C, thereby increasing performance. However, the coatings' absorbance and emissivity are not known at that temperature and might also age more rapidly. They found that high absorbance was achieved (95.3 %) but the expected lifetime still had to be determined.

Most PTCs use oil as the heat transfer fluid in the process. This oil is then used in a steam cycle to produce steam, from which electricity is produced. It is important to know what the thermal performance of a parabolic trough is and Xu *et al* (2014) explored how this could be achieved. They looked at three methods to determine the thermal performance, namely steady state, quasi steady state and the dynamic method. They found that the dynamic method may be a quick, reliable on-site test method. Some papers have been published, investigating whether alternatives to oil as the heat transfer fluid can be used. Alguacil *et al* (2014) looked at direct steam generation, which was found to pose many complications. The process control needs to be more sophisticated to account for saturated steam in the loops, especially during times of transient radiation. They managed to validate a control strategy that guaranteed the stability of a plant even during transitory periods of radiation. They also managed to operate the receiver at 450 °C on a demonstration plant.

The biggest problem PTCs face is irregular energy yield. Electricity demands are typically highest in the late afternoon to evening and PTCs operate at a much lower efficiency then. Worse still, once the sun has gone down, there is no sunlight to concentrate and no energy to be gained. To combat this, PTC power plants are designed to store energy in the form of salt mixtures. An illustration of what a typical CSP plant looks like is taken from Wang (2008) and given in Figure 2-4. As can be seen from the image, the THF can be used to heat up a salt mixture or used for direct steam generation. A similar image was seen in one of Solar Millenium AG (*sa*) documents. In it they describe how during peak hours, the middle of the day, the THF can be used for both heat storage and steam generation. Once the sun sets, the heated salt mixture is used in the steam cycle, thereby enabling the power plant to produce electricity over a 24 hour window. There is a lot of research on molten salts that could be used for thermal storage and Ruegamer *et al* (2014) explore the application of some in a CSP plant. Their results showed that using their salt decreased the levelized cost of electricity by 20 %, significantly increasing the competitiveness of PTCs. Some PTC power plants use gas or biofuels in a sort of hybrid plant if their heat storage is insufficient or cloudy weather prevents the plant from operating as expected. In this way energy losses due to bad weather can be minimised.

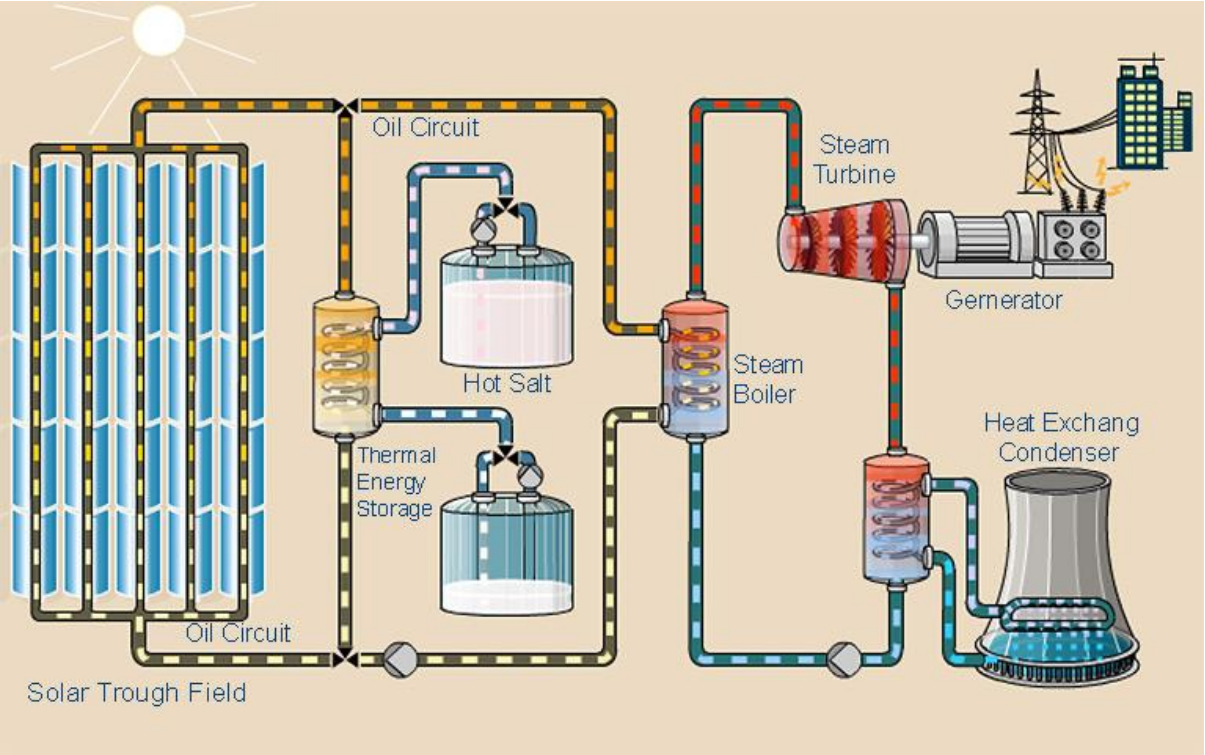

Figure 2-4: Basic process overview of a typical parabolic trough collector power plant (Wang, 2008)

Another important consideration is the effect of wind on the PTCs. Since collectors are mostly out in the open, they are subject to ambient air, as well as loads brought about by wind. Wind can also negatively affect the heat transfer to the receiver. Hachicha, Rodriguez and Oliva (2014) assessed the effects wind might have on a parabolic solar collector. Their main findings included that the heat loss over the heat collector element was typically overestimated, up to 64 %. They also found that turbulence fluctuations are important at inclined positions, which can cause vibrations and stresses. These may lead to structural failure. Interestingly Brooks, Mills and Harms (2006) found that shielding a receiver from wind with glass reduced the heat loss coefficient to half its value. They recommend using a glass shield especially in high wind areas. Garcia *et al* (2014) also explored the effect of wind loads on a PTC. They recommend construction of windbreaks, especially in sandy areas. These consist of a solid wall with a porous fence on top. They protect the mirrors against sand and also reduce the mean aerodynamic loads across the PTCs.

2.4 Linear Fresnel Collector

It was previously mentioned that LFCs are considered an alternative to PTCs. While both technologies have their own advantages and disadvantages, parabolic trough collectors remain the preferred choice, likely due to their slightly better performance. Pitz-Paal (2012) puts the peak solar electricity conversion efficiency for PTCs at 23 – 27 %, while for LFCs he gives a value of 18 – 22 %. An advantage LFCs hold over PTCs is that they require only two

thirds of the area a PTC power plant with the same output would (Morin *et al,* 2012). Other advantages include being cheaper to manufacture, since flat mirrors are produced on large scale. They also require less steel and concrete in the support structure is lighter. In addition to this they are less susceptible to wind loads and have better structural ability. The aperture between the flat mirrors, however, means that energy is lost. The flat mirrors are also susceptible to astigmatism and a secondary mirror is required above the receiver to focus the scattered light onto the receiver. A visual representation of this is given in Figure 2-5 (Meyers, 2012).

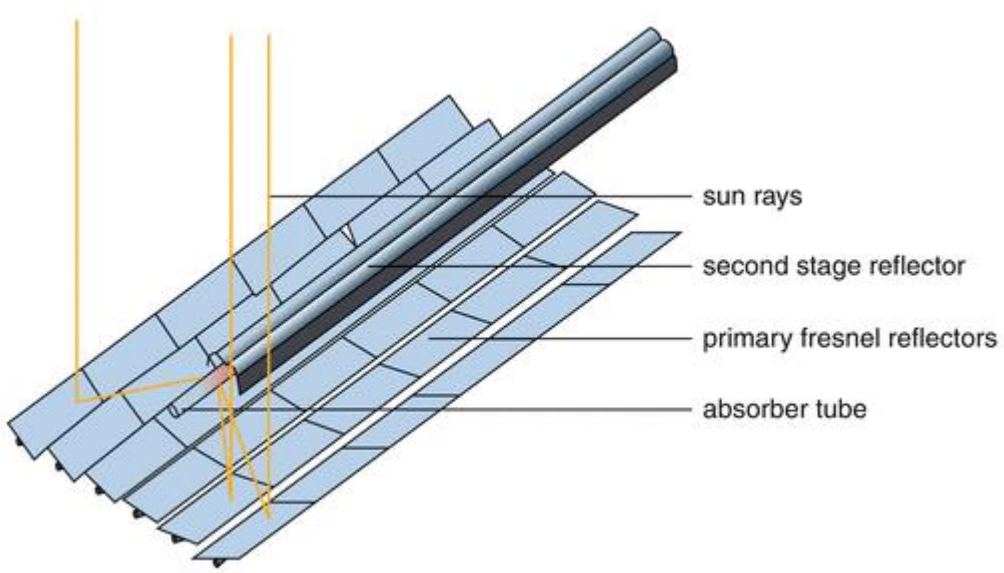

Figure 2-5: Simplified drawing of the design of a linear Fresnel reflector. (Meyers, 2012)

The advantages an LFC power plant offers has prompted more research into the field, as well as solar power plant projects implementing LFCs instead of PTCs. For the sake of a benchmark a technical data sheet about an LFC configuration is consulted. The data sheet is taken from Industrial Solar (*sa*) and found on their website. It lists the following about their linear Fresnel collector LF-11:

- it can generate process heat in the range of 10 kW to 10 MW
- it can operate at pressures up to 120 bar and temperatures up to 400 °C
- its thermal peak output is 562 W/m^2 at suitable conditions based on the primary reflector area
- in terms of installation area usage its thermal output is 375 W/m^2

More information can be found on the technical data sheet, but this is the basic information. A single module consists of 11 mirrors and a total reflector surface area of 22 m^2 which all focus onto a single receiver. The receiver unit includes a secondary mirror to redirect the scattered light. It is suggested these modules are stacked longitudinally, with a recommended minimum row length of 8 modules and a standard row length of 16 modules. This indicates the ability LFCs have to be used on a large scale power plant.

2.5 Solar Irradiance

The sun emits a massive amount of energy in the form of electromagnetic radiation. It is and has been the main source of energy for earth. The flux density that reaches the planet's surface is called the total solar irradiance, or solar constant, and has a value of 1368 W/m^2 (Russel, 2010). Çengel & Ghajar (2011: 709) lists a slightly higher value of 1373 W/m^2. The total irradiance fluctuates during the year as the earth's distance to the sun varies. Taking the world's cross section surface area into account with the solar constant implies that a total 173000 TW are available from the sun. This has prompted great interest in using solar energy as a renewable source since it is so abundant.

However, the world receives this radiation over its entire surface area. Since the world is spherical and not just a flat disc the average solar radiation is only a quarter of the solar constant (342 W/m^2). This value is applicable to perpendicular rays striking the earth's surface. As the world rotates and the sun "sets", the beam of light strikes the earth's surface at an angle. This increases the area that the beam hits, thereby lessening the energy per square metre. This is illustrated in Figure 2-6 below (Russell, 2010).

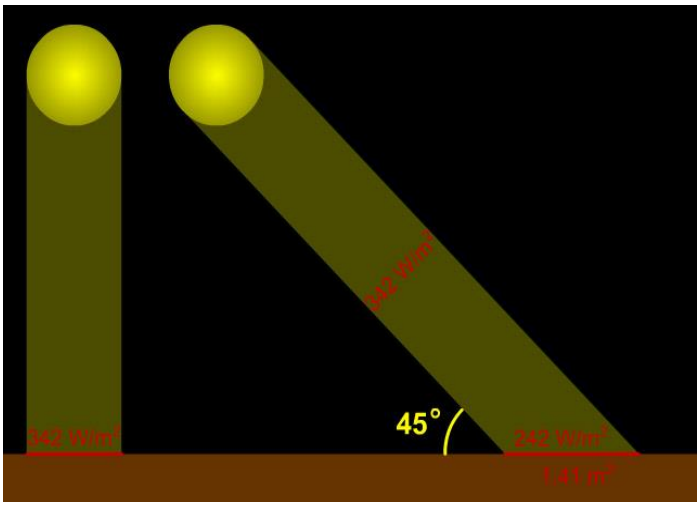

Figure 2-6: Lessening of solar radiation per square metre due to incident light striking the surface at an angle and not perpendicularly. (Russell, 2010)

Different latitudes will receive either more or less concentrated sunlight. As a result, it is important to measure the solar radiation an area receives to be used as a reference point. This is particularly important when calculating the efficiency of a concentrating solar power (CSP) plant.

Dekker *et al* (2012) published a paper on various techniques that can be used to determine the solar irradiance at a point. They express solar radiation as Global Horizontal Irradiance (GHI), which is the total shortwave radiation a surface horizontal to the ground receives from

the sun. It consists of two components, namely Direct Normal Irradiance (DNI) and Diffused Horizontal Irradiance (DHI). DNI comes directly from the sun in a straight line from its position in the sky. DHI does not come in a straight line from the sun, but rather is scattered, mostly due to cloud cover. The following Equation 2-1 relating these terms is taken from Dekker *et al* (2012)

$$GHI = DNI \cos\theta + DHI \tag{2-1}$$

Where θ is the angle the sun makes with the vertical.

The methods Dekker *et al* (2012) explore for the determination of solar irradiation are ground monitoring stations and satellite derived data. The instrument used in ground monitoring is called a pyranometer and can be used to measure GHI, DHI or DNI, depending on its setup. It is recommended that all three terms are measured separately to limit inaccuracies while measuring. Dekker *et al* (2012) found that satellite data over-predicts the solar irradiation, which could have significant setbacks when designing a CSP plant.

2.6 Application in South Africa

Although renewable solar energy has lagged in South Africa, there is a definite growing awareness of the potential large-scale application of it. This is in part due to the ever-growing electricity demands the national provider Eskom has to meet. South Africa is very dependent on coal. About 93 % of the electricity produced in South Africa is coal based (Winkler, 2005).

Because burning coal produces greenhouse gases, a renewable alternative is of great importance to cut down on CO_2 emissions. Unfortunately there is a high tariff for “green” electricity. While it is expected that the costs of producing electricity using renewable methods decreases as more research is conducted, the Industrial Development Corporation (2012) states the costs will have decreased to economically feasible rates by 2030. They report that the cost of electricity generation for CSP should decline to R 0.80 per kWh by 2030. However, this is still more than the coal alternative at an estimated R 0.50 per kWh. An older source (Brooks, 2005) states that the capital cost of a CSP plant would be R 24 000 per kilowatt, compared to R 10 000 per kilowatt for a coal-fired power station. Winkler (2005) compares different policies the government should consider to encourage more use of renewable energy. The conclusion he reaches is that government should set the quantity of “green” electricity that should be produced and let industry find the most cost-effective way of achieving it.

Concentrated solar power is still a young field and as such there is a lot of uncertainty and risk involved. As more research is performed the costs are likely to decrease (IRENA, 2012). South Africa is well suited to CSP plants, because of its high solar irradiation and vast open areas. Local research in this field creates awareness and demonstrates a willingness to invest in the

field. Papers such as Dekker *et al's* (2012) determination of solar irradiation are stepping stones to building large scale plants. Even local research on a parabolic trough solar collector (Brooks *et al*, 2006) aids in reducing risk and uncertainty. Its findings were a significantly lower heat loss coefficient is achieved when the absorber is glass shielded. Fluri (2009) also published a valuable paper in which he identified key areas in South Africa that would lend themselves well to CSP. An image he developed to illustrate the areas of high solar irradiation is given in Figure 2-7 below (Fluri, 2009).

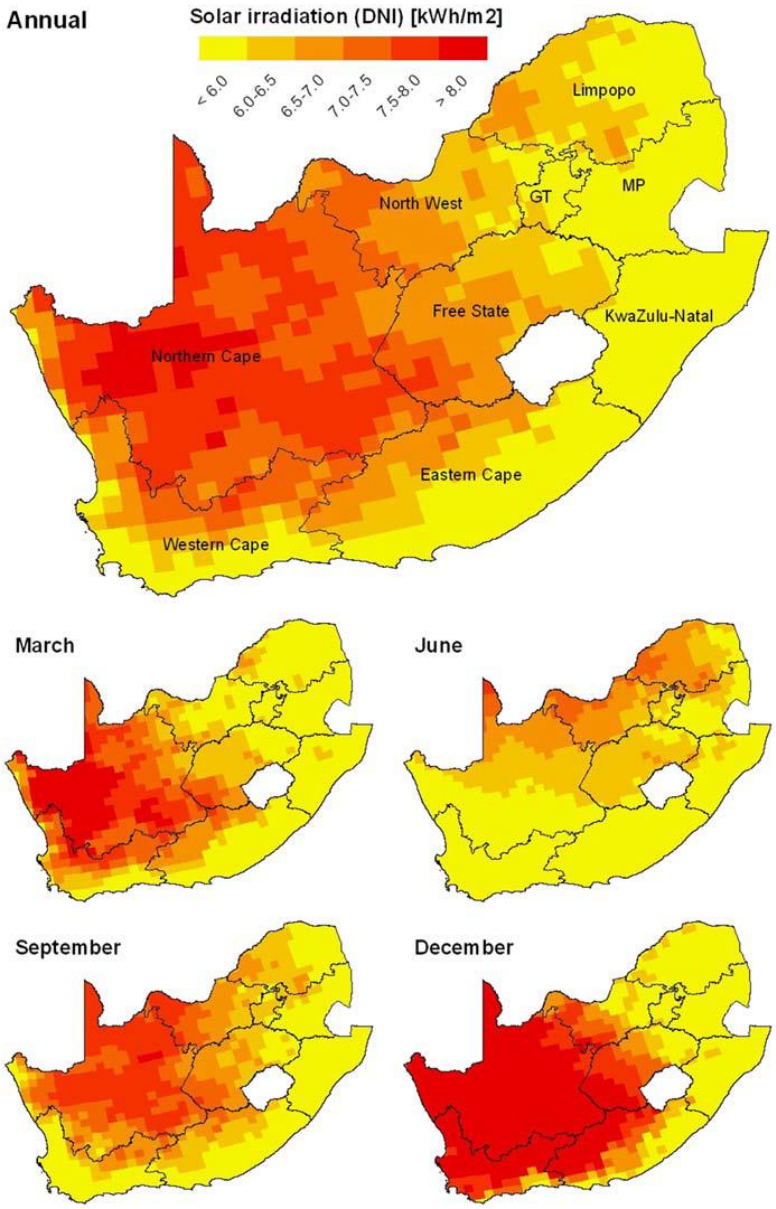

Figure 2-7: Solar Irradiation of South Africa during different times of the year (Fluri, 2009)

The requirements he set out were that the area had to be flat, had to have a high solar irradiation (DNI > 7 kWh/(m^2xday)) and had to be near the local transmission lines. His main findings were that a total of 547.6 GW could be used, mostly in the Northern Cape, but also in the Western Cape, North Western Province and Free State. This type of research and

information is invaluable and a necessity if South Africa is going to make use of large scale concentrated solar power plants in the near future.

2.7 Flow and Heat Transfer Equations

The type of flow through a pipe can be described using the dimensionless quantity, the Reynold's number which is calculated using Equation 2-2 (Çengel & Ghajar (2011: 385))

$$Re = \frac{\rho D v}{\mu} \tag{2-2}$$

Where Re is the Reynolds number, ρ is the density of the liquid, D is the internal diameter of the pipe, v the linear flow rate of liquid through the pipe and μ is the dynamic viscosity of the liquid. The resulting Reynolds number indicates whether the flow is turbulent of laminar. The listed values for most practical purposes are laminar flow at Re < 2300 and turbulent flow at Re > 10 000. In between these two values the flow is considered to be transitional.

When considering heat transfer to a fluid in a circular tube, it is important to start at a general analysis. This is depicted in Figure 2-8 and expressed in Equation 2-3. The fluid in the circular tube receives its thermal flux from the surface of the tube. The thermal conditions at this point can be expressed by one of two fairly accurate approximations. The first is the surface temperature of the tube is constant and the second is the tube is subjected to constant thermal flux.

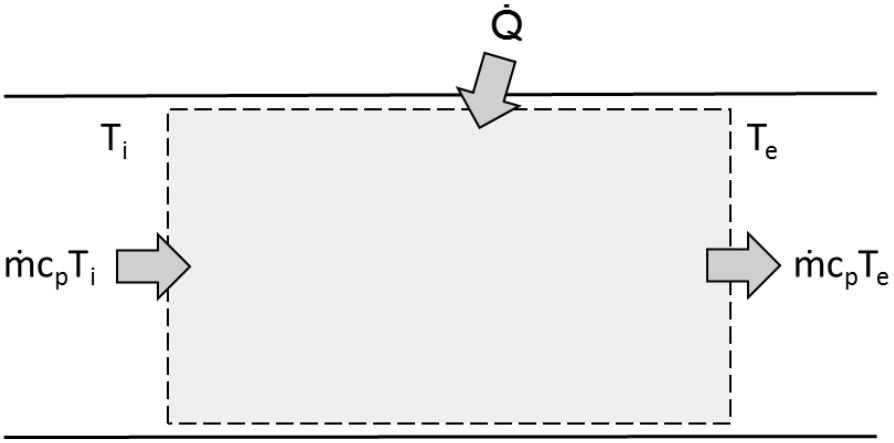

Figure 2-8: Basic thermal analysis of fluid in a circular tube

$$\dot{Q} = \dot{m} c_p (T_e - T_i) \tag{2-3}$$

Where $\dot{Q}$ is the rate of heat transfer to the fluid, $\dot{m}$ is the mass flux of the fluid, c_p is the heat capacity of the fluid and T_e and T_i are the exit and inlet temperatures of the fluid respectively. This Equation can be used to calculate the actual amount of energy transfer, $\dot{Q}_{actual}$, that occurs

in a system with a cylindrical tube. For a pipe that undergoes solar radiation, it is not unreasonable to assume that that the surface flux, $\dot{q}_s$, is constant. In this case Equation 2-4 is used to calculate the expected exit temperature of the fluid (Çengel & Ghajar (2011: 473))

$$T_e = T_i + \frac{\dot{q}_s A_s}{\dot{m} c_p} \tag{2-4}$$

Where A_s is the surface area of the tube. In the case of a solar parabolic trough, the surface flux is a concentrated solar flux, which is dependent on the area of the concentrator that is used. The surface flux and surface area can therefore be replaced by the incident solar flux, $\dot{Q}_{solar,incident}$, which is calculated using Equation 2-5.

$$\dot{Q}_{solar,incident} = (1 - \alpha_{conc})\alpha_{rec} \dot{I} A_{conc} \tag{2-5}$$

Where α is the absorptivity of the concentrator or receiver respectively, İ is the solar irradiance a horizontal surface receives and A_{conc} is the total area of the concentrator that is used. In an ideal case, the concentrator would have an absorptivity value of 0 and the receiver would have an absorptivity value of 1. In this ideal case the entire flux focused onto the receiver is used to heat up the media in a cylindrical tube and any potential losses are ignored. In reality the theoretically expected energy flux can be expressed as in Equation 2-6

$$\dot{Q}_{theo} = \dot{Q}_{solar,incident} - \dot{Q}_{losses} \tag{2-6}$$

Where $\dot{Q}_{losses}$ can be expressed by Equation 2-7

$$\dot{Q}_{losses} = \dot{Q}_{conv,rec} + \dot{Q}_{conv,env} + \dot{Q}_{rad,env} \tag{2-7}$$

Where $\dot{Q}_{conv}$ are the convection losses either from the receiver to the medium or to the surrounding environment, and $\dot{Q}_{rad}$ are the radiative losses to the environment. A generic calculation for $\dot{Q}_{conv}$ is given in Equation 2-8 and for $\dot{Q}_{rad}$ in Equation 2-9.

$$\dot{Q}_{conv} = hA\Delta T \tag{2-8}$$

$$\dot{Q}_{rad} = \varepsilon\sigma A({T_s}^4 - {T_{surr}}^4) \tag{2-9}$$

Where h is the convective heat transfer coefficient, A is the area in question, T refers to temperature, ε is the emissivity of the radiating body and σ is the Stefan Boltzman constant

which is $5.67e10^{-8}$ (Çengel & Ghajar (2011: 21)). The losses are difficult to predict, especially since the receiver is subject to variable wind speeds and therefore variable forced convection. The wind speeds are not measured due to economic constraints, but it is worth considering as this would help create a more sophisticated theoretical model. For the scope of this dissertation the losses are mentioned, but conclusions are drawn from achieved results compared to an ideal case, when losses are negligible. Future runs should consider taking wind measurements and accurately modelling the losses in the system for better analysis.

In order to understand and compare the data that is experimentally achieved, an efficiency in percentage is calculated using Equation 2-10. This equation compares the experimentally obtained value with a theoretically calculated one and was taken from Miqdam Tariq *et al* (2012). It is used as theoretical model in order to compare actual experimental results discussed in subsequent chapters.

$$\eta = \frac{\dot{Q}_{actual}}{\dot{Q}_{solar,incident}} * 100 \quad (2\text{-}10)$$

Chapter 3: Experimental Design

Initially the project was to be carried out on a roof, however, there was insufficient space. An area became available on a field that could house the parabolic trough, also referred to as the rig, as well as a shack for storage and a water reservoir. The GPS coordinates of the setup are -25.750665, 28.261678 and a screenshot of Google Maps can be seen in Figure 3-1. This chapter covers the layout and design of these structures and all relevant connecting pieces. At the end of this chapter the method used to carry out the experiments is explained fully.

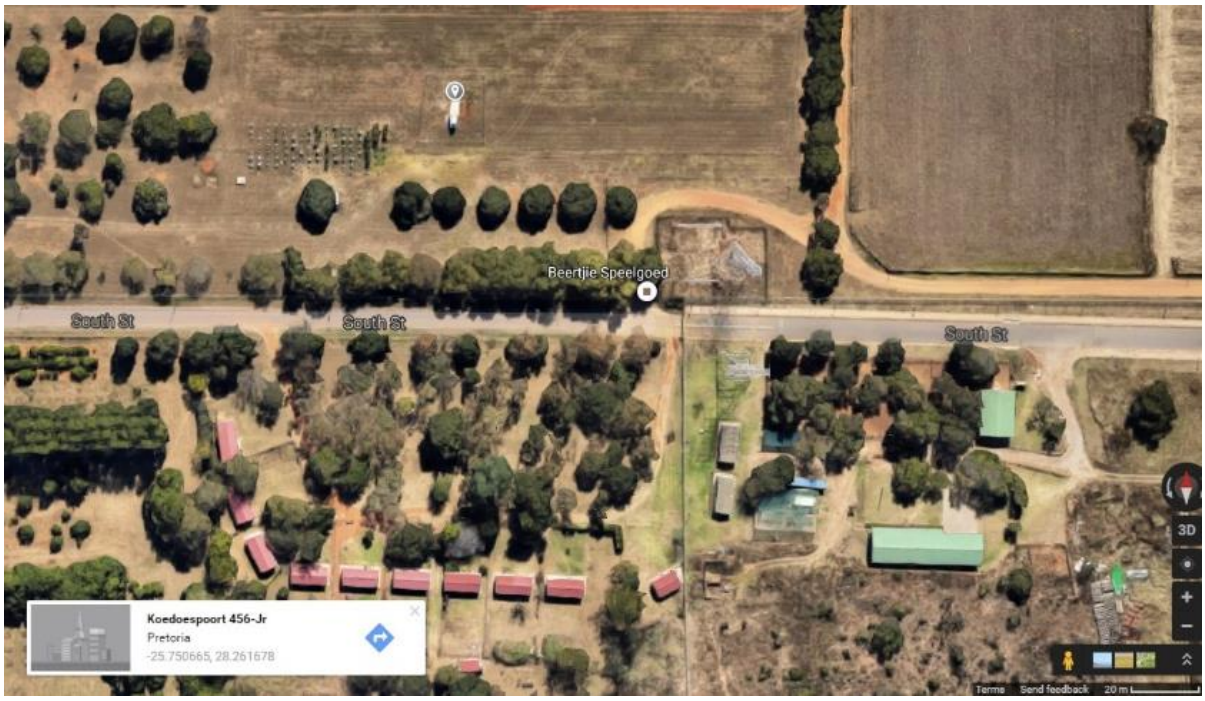

Figure 3-1: Google Earth screen snapshot of the setup's GPS location

3.1 The Rig

The parabolic trough rig was bought pre-designed and unassembled. A simplified isometric drawing of it assembled can be seen in Figure 3-2, while an orthographic view of the front (the North face) is seen in Figure 3-3. The rig consists of a metal frame, which is orientated to be perpendicular to North. Atop of this frame is a 40.9 mm ID pipe, which points to North and is therefore also perpendicular to the frame. The pipe is galvanised steel, is a worn black colour and is 398 mm in length. Attached to the pipe are four metal cut-outs that in the form of pairs create the parabolic support structure for the concentrator. They are attached in a way that allows them to swivel around the pipe in an East-West direction. Clamped onto the metal cut-outs is an iron bar that allows an actuator to move the assembly along the East-West orientation and thereby keep the focal point on the pipe.

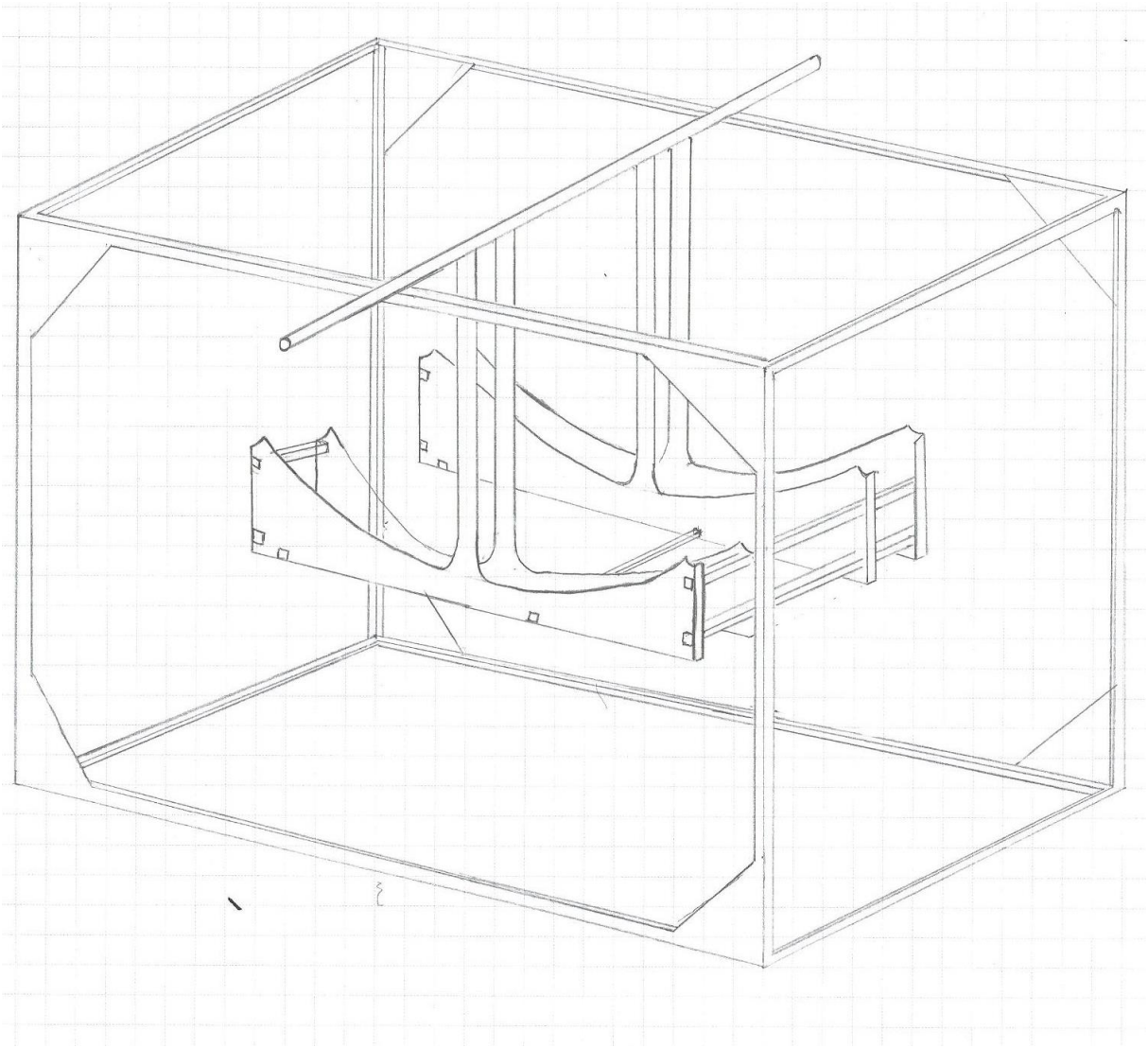

Figure 3-2: Simple isometric drawing of the rig when constructed

The rig was designed to be operate self-sufficiently. Two lead batteries provide power to a 55 W linear actuator, and these are kept at a reasonable charge due to a photovoltaic solar panel. However, since photovoltaic solar panels are expensive and electricity is required to pump water, an economic alternative to power the rig was found in the form of an inverter. The inverter changed the alternating current from the mains into the direct current the actuator required. This was therefore used in the batteries and solar panel's stead.

The rig design also included two black sensors. These would automate the tracking of the rig by following the shadow cast by the black pipe overhead so that it covers half of each sensor. However, multiple instances of the tracking system not aligning correctly, or simply not tracking at all, led to the decision to exclude it. Possible explanations for the failed tracking include, cloud cover, strong sudden gusts of wind and imperfect alignment. Instead the tracking was done manually to mitigate errors and avoid failed runs.

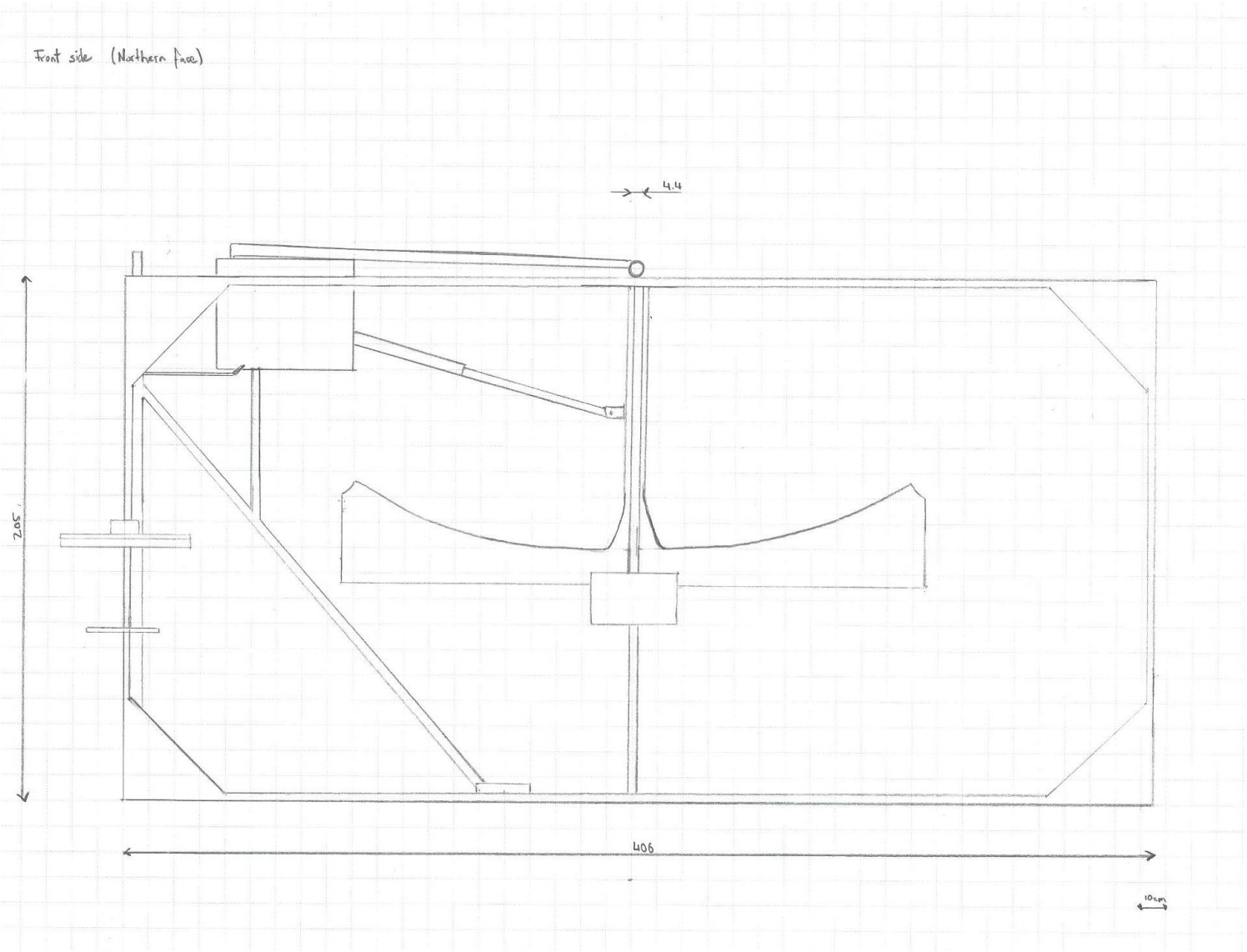

Figure 3-3: Single orthographic representation of the rig's northern face

A photograph of the assembled rig can be seen in Figure 3-4. The rig has the first concentrator, stainless steel metal sheets, attached and the overhead pipe is unpainted. This was the first experimental setup that was tested. The photo also shows the current location of the PTC, namely a testing field.

Figure 3-4: Photograph of the assembled rig on a testing field with metal sheets attached

3.2 Concentrators

Two different types of concentrator were used for comparison. Each was used in two different configurations, namely an unpainted and a painted receiver. This was done to help characterise the PTC, as well as test the effect a matte black, homogenous paint would have on the receiver. The first concentrator tested was stainless steel sheet metal. It was cleaned and polished to try yield its most reflective properties.

The second concentrator was similar to an LFC, namely thin strips of glass mirror. These mirror strips each had the dimension 19 x 1220 mm and were slanted along the metal frame, in a similar fashion to the way Fresnel lenses are slanted. In contrast to an LFC the strips were not moved to track the sun, but rather were fixed and the frame of the rig was moved, like in a PTC application. In this manner each strip focused sunlight onto the pipe overhead. A total of 176 strips were used to completely kit out the rig. A very important characteristic that needs to be considered in solar application is the respective solar absorptivity, α_s, and the emissivity, ε, of materials. Values are taken from Çengel & Ghajar (2011: 890) in order to complete Table 3-1. In an ideal case the concentrator would have a solar absorptivity of 0, while the receiver would have an absorptivity of 1. Some materials are included for reference.

Table 3- 1: List of materials and their solar radiative properties (Çengel & Ghajar (2011: 890))

Material	Solar absorptivity α_s	Emissivity, ε, at 300 K	Ratio α_s / ε
Aluminium polished	0.09	0.03	3
Galvanised sheet metal			
-clean, new	0.65	0.13	5
-weathered, oxidised	0.80	0.28	2.9
Black (Parsons) Paint	0.98	0.98	1
Steel, mirror finish	0.41	0.05	8.2
Steel, heavily rusted	0.89	0.92	0.96

Since solar absorptivity of the concentrator should be as low as possible, it is recommended that the material used as a concentrator should be protected, as well as looked after. Both galvanised steel and steel have a much higher absorptivity value, once rusted or weathered. There was no listed absorptivity value for a glass mirror, however, the Solar Energy Research Institute (1985: 3) states that glass mirrors have a high reflectance between 82 % and 97 %. As such it is assumed that the absorptivity value of a glass mirror would be in the region of 0.18 – 0.03.

3.3 Peripherals and Layout

In order to run water through the parabolic trough collector, flexible hose and galvanised steel are used as connectors. Water is stored in a 1000 L Jojo tank from which the water is siphoned through 25 mm ID PVC garden hose due to a PRA 150 M Ebara pump. The water is siphoned from the very bottom of the tank. This design has the major drawback that suction can reduce the flow of water through the pipe and cavitation can easily occur. Care also needs to be taken to ensure the pump is properly primed before switching it on. However, the advantages are a much easier installation and no permanent holes are drilled into the storage tank.

At the exit point of the pump is more of the flexible hose which leads to a plastic T-piece. The T-piece feeds most of the pumped water directly back into the tank via a fully opened throttling valve and more flexible hose. This allows a slower and more controlled flow rate through the PTC. The other pathway from the T-piece leads to a metal throttling valve that serves as the fine tuning element for setting the flow-rate. In order to better visualise the explanations given, photographs are included in Figure 3-5 and Figure 3-6.

The throttling valve has an internal diameter of 25 mm and is set to 1/8th from closed. This enables a satisfactory flow rate through the parabolic collector. After the throttling valve galvanised steel pipes with an ID of 25 mm lead to and from the rig. In total 40.2 m of galvanised steel are used and there are eight 90° elbows. Of those three are before the PTC and five are after, leading back to the water tank. Similarly 18.6 m are used before the PTC and 21.6 m complete the system.

Figure 3-5: Image of the water reservoir and the PVC hose pipe that leads down to the Ebara pump and back up to the tank

Figure 3-6: PVC hose pipe connecting to a throttling valve that controls flow through the PTC

The P & ID shows the six thermocouples that are used to take temperature measurements and where they are situated. They are named after the measurement they take, namely: IN, OUT, RECEIVER, CONCENTRATOR, TANK and AMBIENT. These six measurements are chosen to characterise and better understand the system, and more importantly, the parabolic trough collector. Hence four of the six thermocouples take a reading on the PTC. The thermocouples are K-type and all use their original wiring, except for “IN”, which needed an extension as it was furthest away. The thermocouples are connected to a National Instruments NI USB-9213 DAQ, which in turn is connected to a laptop for data logging purposes. According to the user guide and specifications document of the DAQ, temperature measurement sensitivity is limited to <0.02 °C (National Instruments Corporation, 2009). The standard limits of a typical K type thermocouple have tolerance values of 2.2 °C or 0.75 % (OMEGA, *sa*). The data is logged on National Instruments software LabVIEW™ 2013 edition.

The thermocouples “IN” and “OUT” are installed by drilling small holes into the ends of the black pipe of the rig. They are inserted so that their tips are in the middle of the pipe, then held in place and sealed off using silicone. They are spaced 267 mm apart, so that they encapsulate as much of the concentrated sunlight as possible. A third hole is drilled at the top end of the black pipe to ensure the system is pressurised and water fills the pipe completely. This hole is sealed with a clamp. To illustrate better the layout of the entire system a simple P & ID is shown in Figure 3-7.

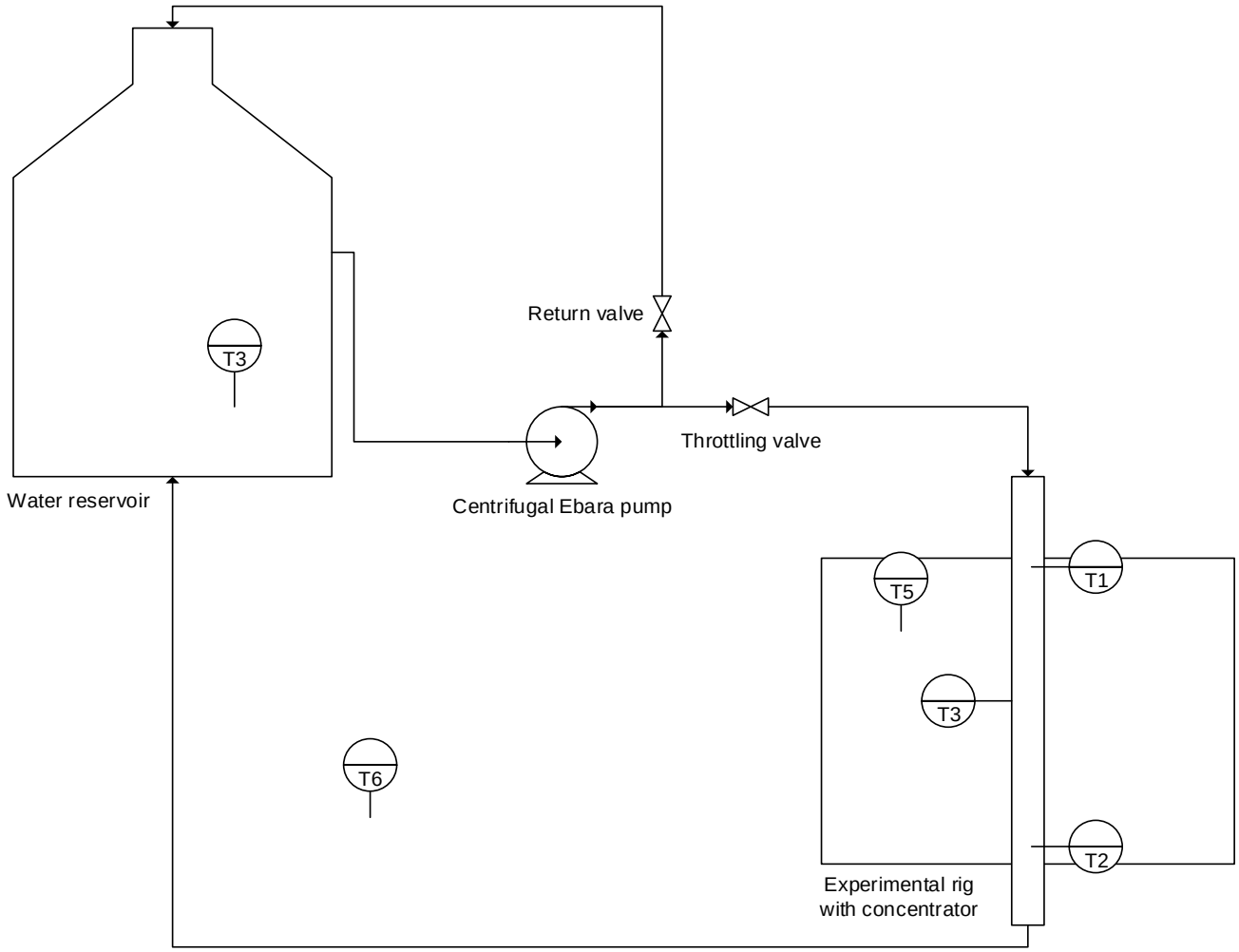

Figure 3-7: P & ID of the experimental setup

The other thermocouples are fastened so that they are in contact with the material they are measuring. The thermocouple “TANK” is submerged in the tank close to the bottom to ensure the reading is of water in the tank and not the hot water that is fed to the top of the tank. For similar reasons the hosepipe that siphons the water is placed right at the bottom of the tank. A pyranometer is used to measure the irradiance for comparative purposes, as data is also taken from South African Universities Radiometric Network (SAURAN). The station that logs the data is about 3.6 km away which is measured using Google maps, as seen in Figure 3-8. This distance is for all practical purposes considered negligible, however, a comparison with locally gathered data is considered useful.

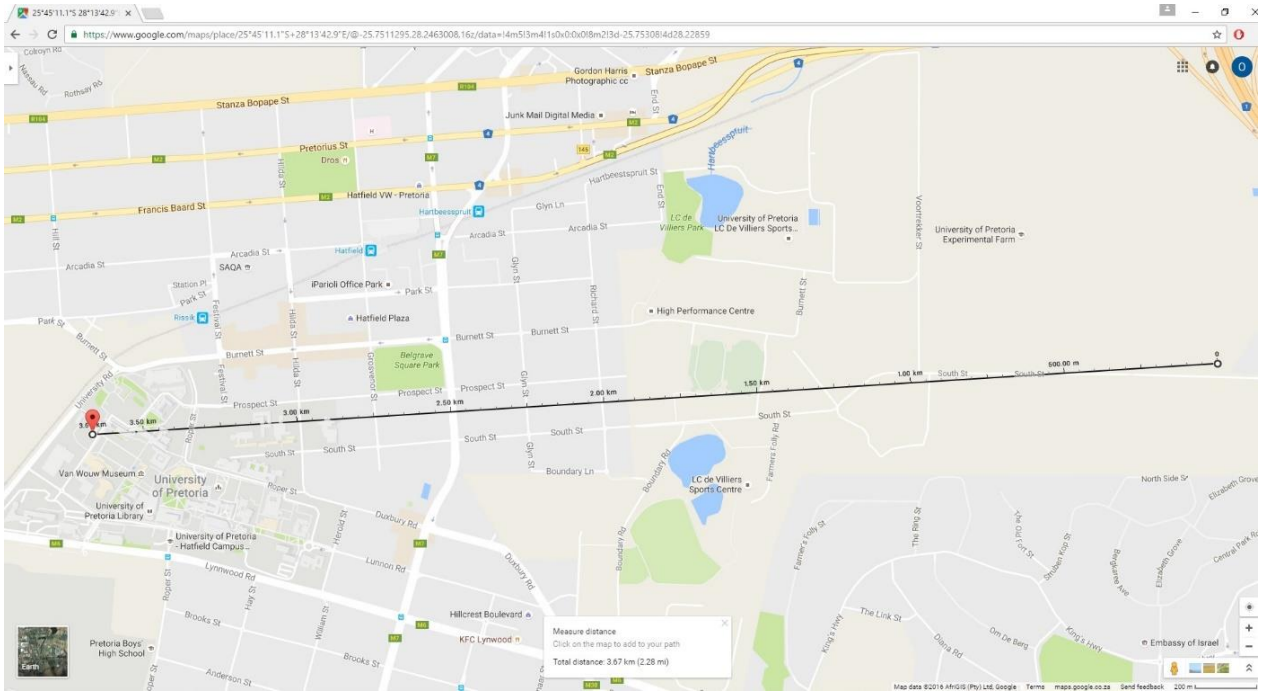

Figure 3-8: Google Maps screen shot of the distance between SAURAN data collector and experimental setup - 3.6 km

3.4 Flow Rate

The flow rate was manually set by completely opening a throttling valve after a T-piece that enabled a return stream to the water tank immediately after the pump. Then a second throttling valve was set so that a desired flow rate was achieved. The final setting of the second throttling valve was 1/8th open. After this the flow rate was measured using a measuring jug over various time intervals. The flow rate was measured repeatedly on different days to ensure an average with improved accuracy would be achieved. Some results are given in Table 3-2. The average flow rate was calculated to be 0.08 m^3/h.

Table 3-2: Logged volumes of water over time in order to determine the volumetric flow rate.

Time (s)	Volume (L)	Volumetric Flow Rate (m^3/h)
9.91	0.23	0.080
10.25	0.22	0.077
29.99	0.6	0.072
30.57	0.75	0.088
30.14	0.62	0.074
40.3	0.98	0.087
60.06	1.28	0.077
59.98	1.27	0.076
120.18	2.91	0.087
120.08	2.61	0.078

Given the internal diameter of the black pipe is 40.9 mm and using Equation 2-2 the Reynolds number was calculated to be 768.7. This number is well below 2300 and therefore the region considered laminar. As previously mentioned, a hole at the end of the pipe was used to ensure that flow through the pipe was fully developed. A list of the relevant characteristics for the flow through the pipe is given in Table 3-3. The flow rate through the pipe is much lower than the pipe's minimum capacity. This is achieved by feeding most of the pumped water directly back into the reservoir. The pump curve for the pump in question is given in Appendix 1.

Table 3-3: List of flow characteristics

Description	Value	Unit
ID of pipe	40.9	mm
Average Volumetric Flow Rate	0.079	m^3/h
Cross sectional area	0.0131	m^2
Linear Flow Rate	0.017	m/s
Viscosity of water	0.00089	Pa.s
Reynolds	768.7	-
Friction factor	1.7	-
Length of galvanised steel used	40.2	m
Number of Elbows used	8	-

3.5 Experimental Procedure

The experiments are broken down into three separate runs. Each run is meant to last an hour and fifteen minutes. This interval is arbitrarily chosen, however, it is worth noting that after an hour and twenty-five minutes, LabVIEW™ would start overwriting the first entries of the logged data. This means there was a limit to the number of data points that could be exported from LabVIEW™ at a time. The chosen interval falls well within that range.

The first interval is chosen to start at 10:30 am and last until 11:45 am. This is chosen so that the second run includes time before the peak of the day, namely noon. The second run is thus from 11:45 am till 1:00 pm. This also enables raw data to be exported in the format of a bitmap file directly from LabVIEW™ that coincides with the start of the second run. The bitmap file is the data collected between 11:45 am and 12:15 pm, as this is considered to be the most relevant time of day. The third and final run is from 1:00 pm until 2:15 pm. Measurements in LabVIEW™ are taken every 5 seconds and exported to Microsoft Excel for further analysis. The values reported are the difference between the thermocouple IN and OUT, as well as minimum or maximum values of each run. A trend line is fitted for the logged data using the built in function "LINEST" in Microsoft Excel. This function returns an array with various values, including a slope, an intercept and a standard deviation, which aid in better understanding the gathered data.

Chapter 4: Data Collection

So that a good structure and simplistic overview are achieved, comparison and discussion of the data collected are left for the ensuing chapter. This chapter solely focuses on the different arrangements for the system and the data gathered in those arrangements. There are two variables that were changed, thus creating four different arrangements. The first is the type of collector used, either stainless steel sheets or strips of glass mirror. The second is using the unpainted, faded black pipe or a pipe painted with a semi-matte black paint. In order to help visualise these configurations a graphic of the different arrangements is given in Figure 4-1.

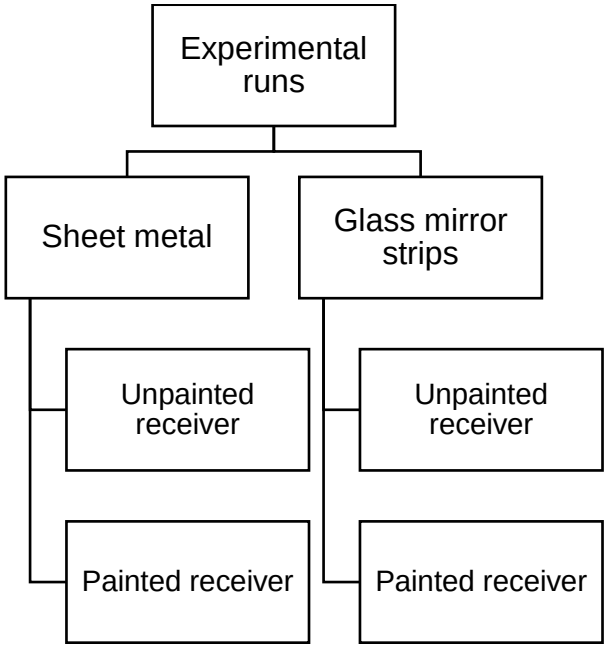

Figure 4-1: Graphic representation of the various experimental setups tested

4.1 Metal Sheets, Unpainted Pipe

The raw data exported from LabVIEW™ using its built-in export function is given in Figure 4-2. This figure shows steady state data logging over the time period 11:45 am – 12:15 pm. This window was chosen as the most significant as the sun is it its highest point and is therefore closest to normal with the earth. In Figure 4-2 amplitude of the thermocouple is plotted against time. A legend to better understand the figure is given in Table 4-1. This legend applies to all graphs in this chapter that are exported from LabVIEW™. In Figure 4-2 a significant difference can be seen between the TANK and IN measurements. This could be due to stratification in the tank, or more likely energy gained by the water in the galvanised steel pipes on its way to the inlet of the receiver.

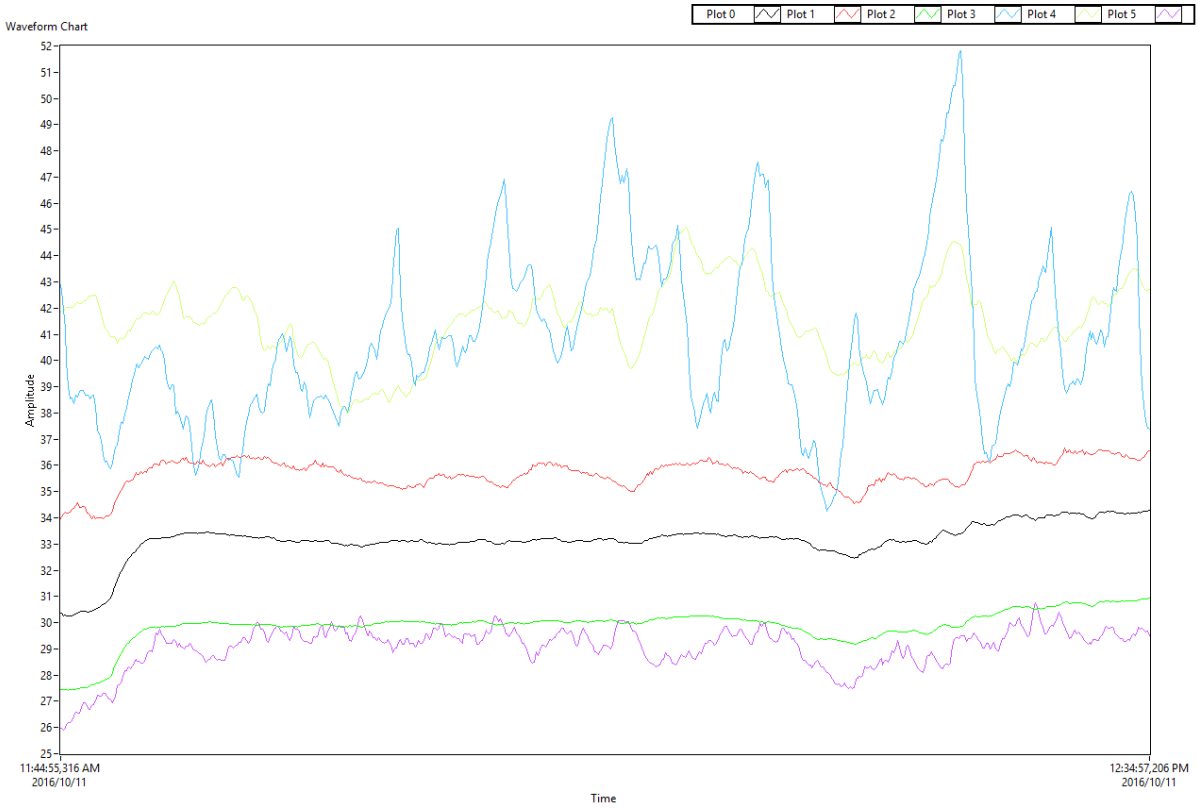

Figure 4-2: Raw data of stainless steel metal sheet from 11:45am – 12:15pm on the 11th of October 2016

Table 4-1: Legend for the exported image file from LabVIEW™

Plot	Description	Colour
Plot 0	IN	Black
Plot 1	OUT	Red
Plot 2	TANK	Green
Plot 3	RECEIVER	Blue
Plot 4	CONCENTRATOR	Yellow
Plot 5	AMBIENT	Purple

As can be seen from the figure the surface temperature of the pipe (receiver – blue) fluctuates significantly. This is likely due to the fact that some irradiance hits the thermocouple, thus causing the measurement to sporadically jump. The remaining thermocouples are relatively stable and the delta T of the inlet and outlet temperature of the water is between 2-3° C. A graphical representation of the expected outlet temperature in an ideal case with no losses versus the actual outlet temperature is given in Figure 4-3. For both data sets a linear trend line is added. The theoretical outlet data in green is calculated using Equation 2-4 and ignores all losses. The actual data is in red, as was the case in the previous image. The time at the bottom of the axis refers to the time of the day. For the theoretically calculated values the absorptivity of the concentrator was taken to be 0.4 and the absorptivity of the receiver (pipe) was assumed to be 0.6. The area of the stainless steel metal sheets is 5.17 m^2 which is a necessary input to calculate the theoretically expected value.

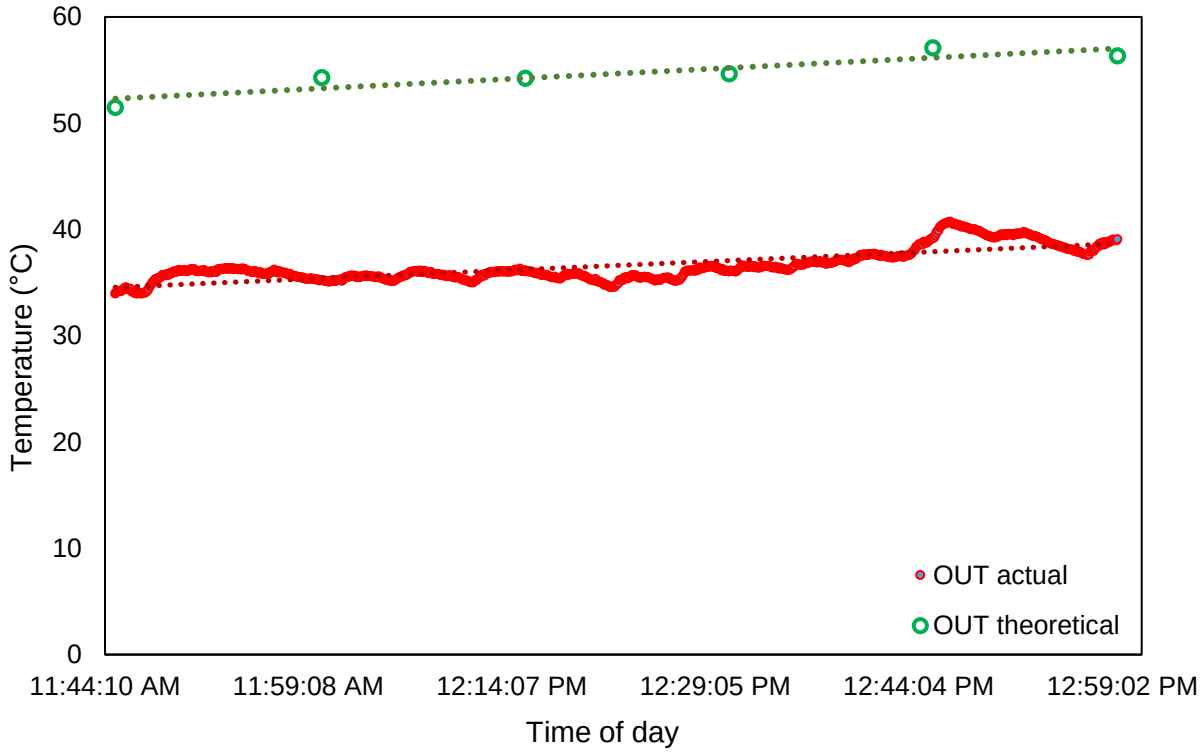

Figure 4-3: Temperature vs time of day graph of the actual outlet temperature and the theoretical outlet temperature for the configuration sheet metal, unpainted receiver

The figure shows that if losses are not present in the configuration the temperature of the outlet water would be almost 20 °C warmer. Having no losses is an unrealistic approximation, but it shows that there is potential to minimise losses and achieve higher exit temperatures. One method to minimise losses is to create a vacuum around the tube and insulating it by means of a glass shield. The assembly in question has no such systems in place. In each case the trend line shows that the system slowly gains energy, as the outlet temperature rises linearly with time. In total there are nine runs for this setup. Their data has been processed and is represented in Table 4-2 for further comparison.

For each run averages, represented by “Avg”, were used in order to better represent the findings and account for any sporadic readings and/or outliers. The properties reported in the table are: the average temperature difference of the inlet and outlet of water in the pipe; the maximum temperature difference of the outlet and inlet; the average ambient temperature during a run; the average surface temperature of the receiver; the average temperature of the concentrator used; the temperature of the water in the tank reservoir at the beginning and end of the run; the actual amount of energy supplied to the system; the average global horizontal irradiance taken from sauran.net; the theoretical energy that could be supplied to the system and the efficiency of the setup.

While the table displays a lot of data, it reveals a lot about the configuration. The temperature of the metal sheets is almost always on average hotter than the pipe surface temperature.

Over the course of a run it is possible to see that the system slowly gains energy. This is evident from the change in temperature of the tank temperature. For this configuration in all cases the run at the end of the day achieved the best results. This may be due to the system operating at a much smoother rate after the initial two runs. Apart from the runs done on the 25th of October, which seem to be an outlier, a typical ΔT of 2 °C – 4 °C is seen and the overall efficiency varies between 8.1 % and 20.8 %. The energy supplied to the water was generally low, ranging from 154 W to 345 W, if one discounts the results by the outlier. The outlier could be the consequence of several variables including, measurement inaccuracies, a lower flow rate, lower ambient temperatures and higher wind velocities interfering with the measurements. The standard deviation for all data is given in Appendix 2.

Table 4-2: Averaged data for all experimental runs for the configuration metal sheets, unpainted receiver

Date	**2016/10/11**			**2016/10/12**			**2016/10/25**		
Time	10:30-11:45	11:45-13:00	13:00-14:15	10:30-11:45	11:45-13:00	13:00-14:15	10:30-11:45	11:45-13:00	13:00-14:15
Avg ΔT (°C)	1.67	2.41	2.67	2.79	3.51	3.75	5.15	6.80	7.04
Max ΔT (°C)	6.51	4.21	3.55	3.97	4.35	5.25	7.81	8.21	8.81
Avg T_{AMB} (°C)	26.91	30.10	32.40	30.71	35.54	33.72	29.60	29.13	30.34
Avg T_s (°C)	37.71	42.29	44.50	40.92	45.88	44.94	42.37	45.10	47.31
Avg T_{CONC} (°C)	39.13	42.72	44.83	42.27	47.73	47.64	41.88	41.70	47.16
T_{TANK} start (°C)	26.90	27.45	33.01	30.36	32.39	34.44	25.93	29.77	31.25
T_{TANK} end (°C)	27.58	33.03	35.43	32.38	34.45	36.35	29.77	31.24	34.05
$\dot{Q}_{actual}$ (W)	153.8	222.1	245.9	256.5	323.1	344.5	474.7	625.4	647.5
Avg GHI (W/m^2)	1014.7	1026.8	920.0	940.6	1008.5	891.9	1045.7	1053.3	947.7
$\dot{Q}_{theo}$ (W)	1889	1911	1711	1751	1877	1660	1946	1960	1764
η (%)	8.1	11.6	14.4	14.7	17.2	20.8	24.4	31.9	36.7

4.2 Mirror Strips, Unpainted Pipe

In this configuration the only variable that was changed was the concentrator. This means that the absorptivity of the receiver remained at a conservatively estimated value of 0.6. However, mirrors are far more reflective than a stainless steel sheet and their absorptivity is assumed to be 0.2. As in the previous section, data was exported from LabVIEW™ in the form of a bitmap image. This image illustrates part of a run over the time period 11:45 am to 12:15 pm and took place on the 27th of October. The image is given in Figure 4-4 and uses the same legend that was given in Table 4-1. The area the mirror strips provide for concentrated sunlight is slightly less than the metal sheets at 4.08 m^2.

The temperature of the concentrator, in this case the glass mirrors (yellow), is much lower and far more stable. This indicates that, as expected, the glass mirrors have a much lower absorptivity value. The surface temperature of the pipe (blue) is more stable than was seen in the sheet metal assembly, however, there are still great fluctuations. This can again be attributed to the effect of solar radiation striking the thermocouple, but occurs to a lesser extent when using glass mirrors. The waveform temperature trend of the outlet temperature (red) can

be attributed to error in manual tracking, as the rig is only moved every few minutes. This means the concentrated sunlight does not always hit the focal point it should be striking. If a functional tracker is used, this error can be avoided. A constructed graph of the runs actual temperature versus a theoretically calculated value is given in Figure 4-5.

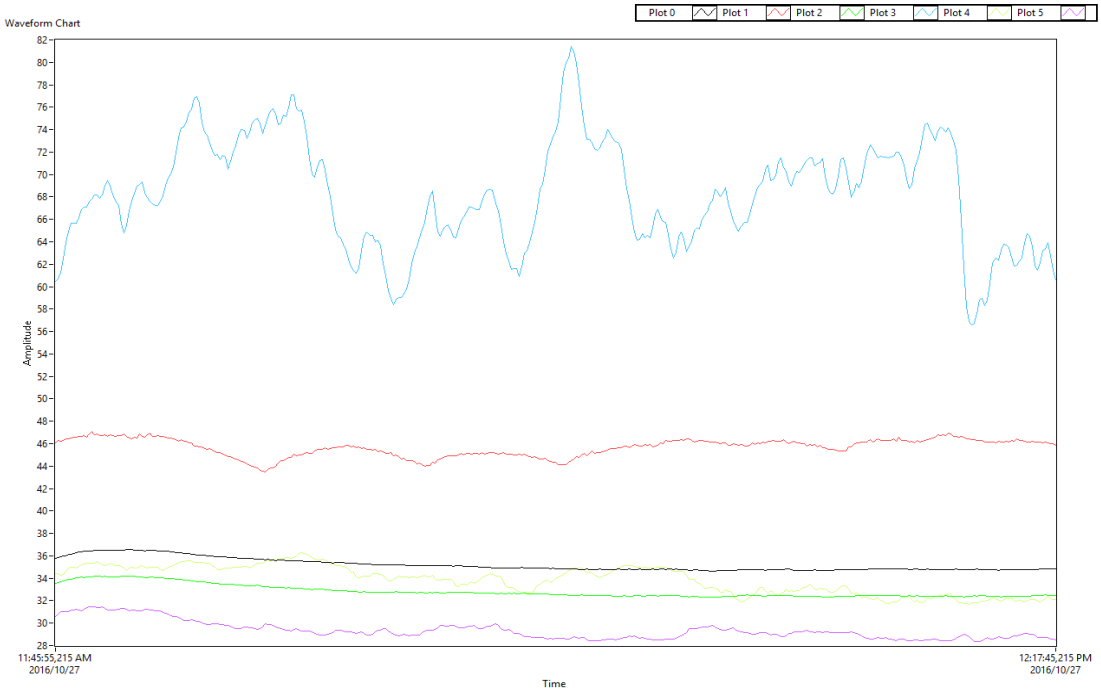

Figure 4-4: Exported image file from LabVIEW™ for the experiment conducted on the 27th of October 2016 for the configuration glass mirror strips, unpainted receiver

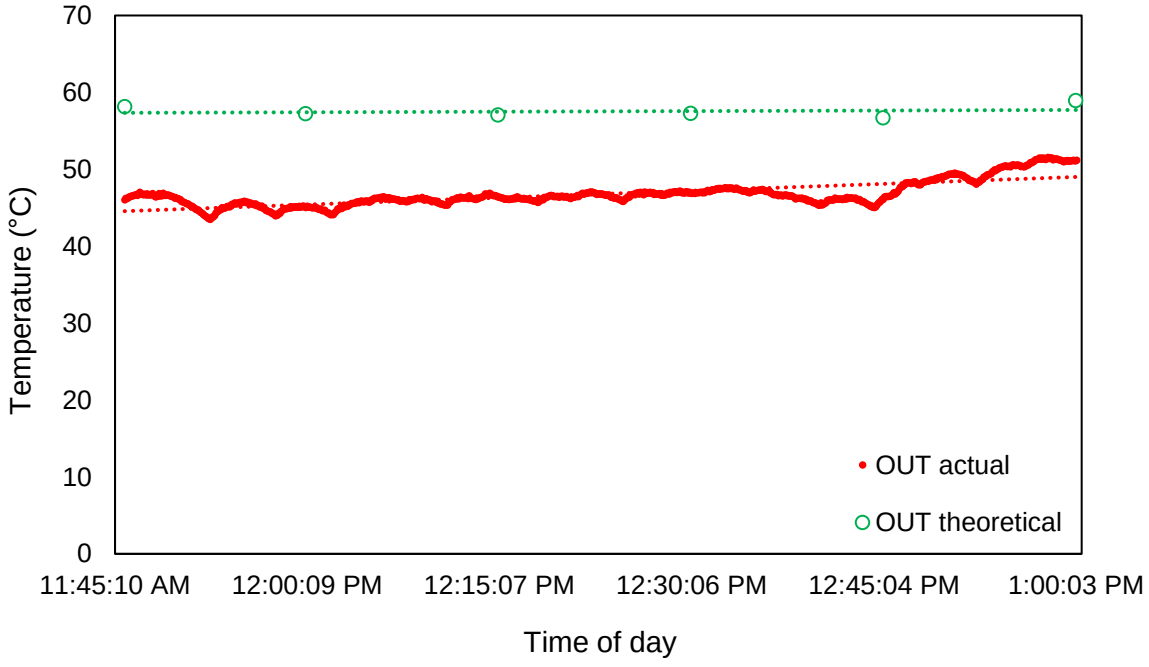

Figure 4-5: Temperature vs time of day graph of the actual outlet temperature and the theoretical outlet temperature for the configuration glass mirrors, unpainted receiver

The Figure shows that the glass mirror strips are quite efficient, as there is not as great a difference between the actual value and the theoretically expected value. In addition to this the theoretical value ignores all potential losses. This means that either the system is running at a near optimum level, or the theoretical value calculated is too conservative and greater improvements are possible. A full representation of the data from all eight runs pertaining to this configuration is given in Table 4-3. As in the previous section average values are reported.

Table 4-3: Data averaged for each experimental run conducted with the configuration glass mirrors, unpainted pipe

Date	**2016/10/26**			**2016/10/27**			**2016/10/28**	
Time	10:30-11:45	11:45-13:00	13:00-14:15	10:30-11:45	11:45-13:00	13:00-14:15	10:30-11:45	11:45-12:30
Avg ΔT (°C)	8.23	10.48	12.06	9.67	11.42	14.13	12.94	12.36
Max ΔT (°C)	12.29	12.93	13.76	11.88	14.32	15.96	14.54	13.77
Avg T_{AMB} (°C)	26.89	28.37	29.47	26.64	29.03	30.86	28.61	29.37
Avg T_s (°C)	52.33	53.06	51.83	65.06	66.83	65.37	58.72	62.62
Avg T_{CONC} (°C)	30.60	31.82	32.35	31.73	33.11	34.08	33.86	34.54
T_{TANK} start (°C)	27.29	29.53	31.29	28.80	33.56	34.85	31.99	33.90
T_{TANK} end (°C)	29.37	31.22	33.74	33.45	34.77	36.19	33.89	35.54
$\dot{Q}_{actual}$ (W)	756.3	963.2	1108.8	889.4	1050.1	1299.7	1189.9	1136.7
Avg GHI (W/m^2)	975	969.3	924.2	1028.5	1031.5	920.7	1029.1	1044.8
$\dot{Q}_{theo}$ (W)	1910	1898	1810	2014	2020	1803	2015	2046
η (%)	39.6	50.7	61.3	44.2	52.0	72.1	59.0	55.6

The Table confirms the graphical findings and interpretations. The surface temperature of the mirror strips is generally low and only a few degrees higher than the ambient temperature. This shows that the mirror strips do have a low absorptivity. The average temperature difference between the inlet and outlet is typically close to or greater than 10 °C. The energy supplied to the system is quite significant, since the values range between 750 W and 1300 W. The efficiencies achieved were also quite high, ranging between 40 % and 72 % respectively.

4.3 Metal Sheets, Painted Pipe

After painting the receiver with a semi matte black paint it was assumed the absorptivity of the pipe increased. A conservative value of 0.8 was used and the absorptivity of the concentrator was assumed to have remained at 0.4. The area of the concentrated light reflected on the pipe was again 5.17 m^2 and these values are used for all calculations in this section.

A first insight into the configuration is given by the exported image file in Figure 4-6. This Figure represents the run that took place on the 28th of November over the same time period as the previous Figures of its type. It shows a similar trend to Figure 4-1, whereby the surface temperature of the receiver is lower than the temperature of the concentrator. The difference in the inlet and outlet temperature seems to a slightly higher with an expected value of 3-4 °C. The legend for the Figure is represented in Table 4-1, see above.

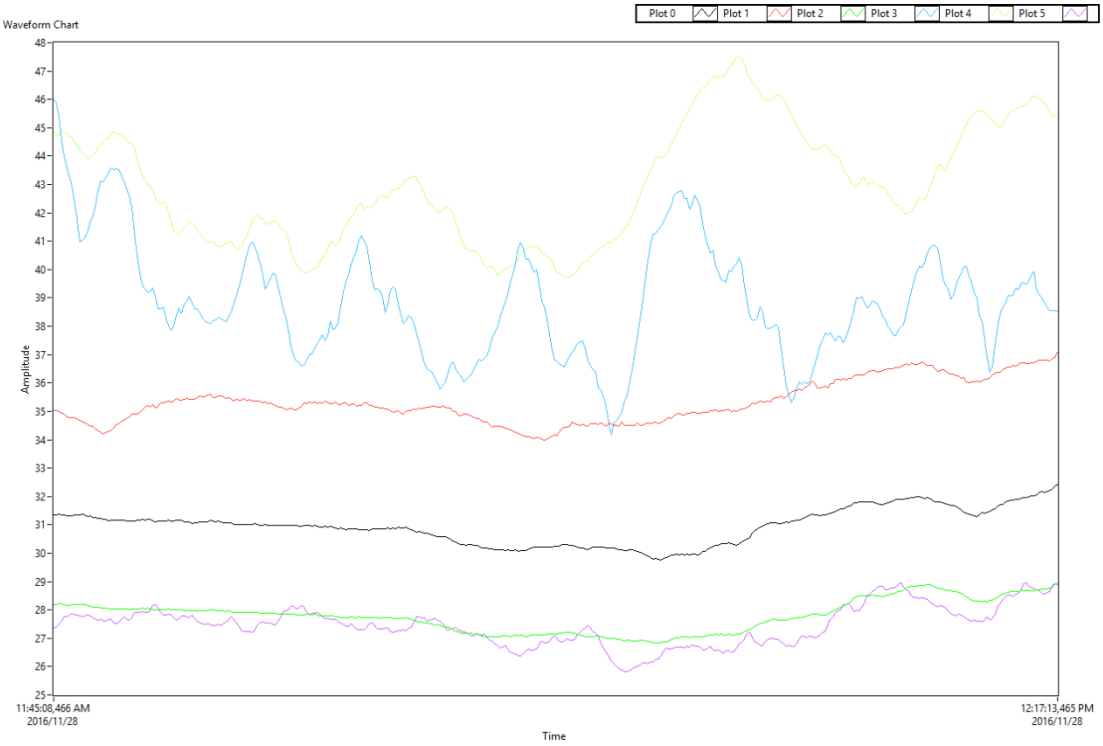

Figure 4-6: Image file exported from LabVIEW™ of an experimental run conducted on the 28th of November when using a painted receiver and stainless steel metal sheets

For the same a run an analysis of the actual outlet temperature compared to the theoretically achievable outlet temperature is given in Figure 4-7. In the Figure the mean difference between the two is approximately 30 °C. This indicates that the efficiency is poor and there are significant losses that are not accounted for. As in the previous graphs of this type a trend line is added for both sets of data. This line slopes slightly upwards over time which is expected.

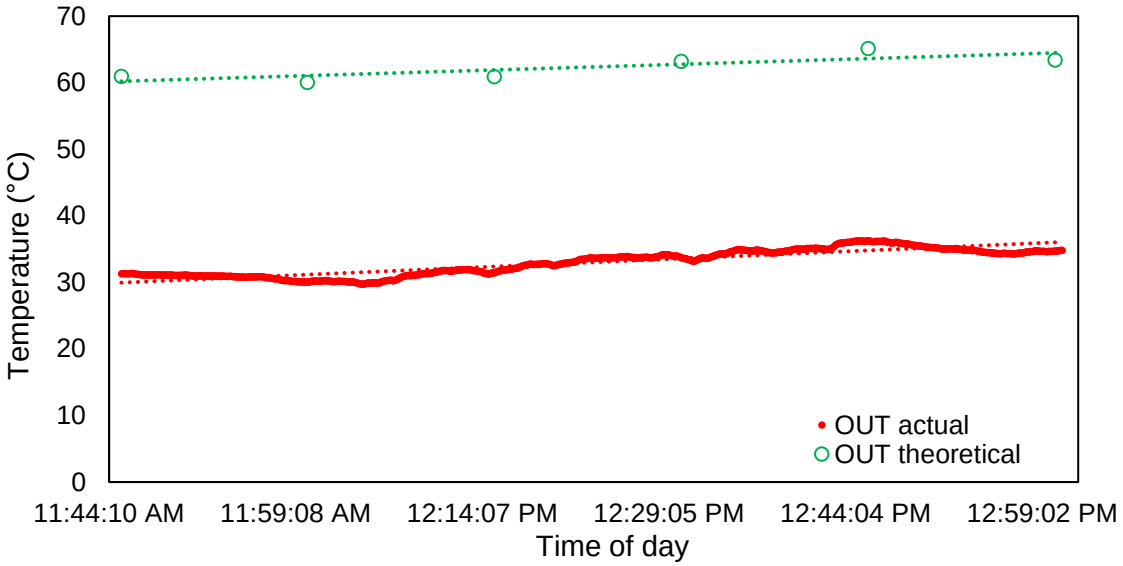

Figure 4-7: Temperature vs time of day graph of the actual outlet temperature and the theoretical outlet temperature for the configuration sheet metal, painted receiver

A complete analysis of the data is available in Table 4-4. There were in total nine runs for the configuration and the Table allows a quick comparison of them. In this data set the very first run could be considered an outlier, potentially due to external interferences and is therefore excluded. Otherwise a fairly uniform result is achieved. Typically the ΔT achieved is around 3.6 °C but varies from 2.1 °C to 4.9 °C. The surface temperature of the pipe is typically 43 °C which is lower than the average temperature of the metal sheets at 48 °C. The effects of heating the water can be seen on the system in the increase of the reservoir temperature over time. However, due to the low ΔT that were measured, the energy supplied is generally low. The actual energy supplied had a maximum value of 450 W, but the average was 332 W. As such the efficiencies achieved were also low, ranging from 6 % to 18 %, but averages 13 %.

Table 4-4: Averaged data for the runs with the setup metal sheets and a painted receiver

Date	**2016/11/18**			**2016/11/28**			**2016/11/30**		
Time	10:30-11:45	11:45-13:00	13:00-14:15	10:30-11:45	11:45-13:00	13:00-14:15	10:30-11:45	11:45-13:00	13:00-14:15
Avg ΔT (°C)	1.83	2.12	4.89	4.19	4.25	3.43	3.40	3.53	3.12
Max ΔT (°C)	3.62	4.45	6.69	5.22	5.03	4.87	5.01	4.22	4.24
Avg T_{AMB} (°C)	29.62	30.26	32.40	28.24	29.21	31.38	30.41	32.06	33.74
Avg T_s (°C)	37.68	41.33	46.51	42.11	41.48	44.29	40.09	42.34	46.34
Avg T_{CONC} (°C)	48.20	48.49	51.37	45.36	45.76	48.72	42.02	44.49	48.50
T_{TANK} start (°C)	30.78	30.99	32.61	27.93	28.19	30.86	28.52	33.85	33.39
T_{TANK} end (°C)	30.99	32.59	36.28	28.13	30.90	34.78	33.84	33.41	36.64
$\dot{Q}_{actual}$ (W)	167.9	194.9	449.2	385.3	391.2	315.1	312.8	325.0	287.0
Avg GHI (W/m^2)	1104.6	1095.3	1004.4	1072.6	1087.3	928.7	1068.7	1081.2	998.9
$\dot{Q}_{theo}$ (W)	2741	2718	2493	2662	2698	2305	2652	2683	2479
η (%)	6.1	7.2	18.0	14.5	14.5	13.7	11.8	12.1	11.6

4.4 Mirror Strips, Painted Pipe

The fourth and final configuration was using the discretised mirror strips in conjunction with the painted receiver. The absorptivity value of the concentrator was 0.2 and that of the receiver was 0.8. This configuration had the lowest concentrator absorptivity and the highest receiver absorptivity, therefore the best results were expected. Figure 4-8 shows for the duration of 30 minutes a run started at 11:45 am on the 17th of November. The Figure is a representation of amplitude versus time and the applicable legend can be seen in Table 4-1 above. From the graph a difference in inlet and outlet temperature of 12 °C can be seen. An unusual occurrence is the fact that the inlet, outlet and tank temperature decreased slightly over time, where typically a marginal increase would be expected. This could be due to mixing in the water reservoir and indicates that only a pseudo steady state was reached. The temperature of the glass mirrors is again low, while the pipe's surface temperature is high. The latter, however, shows violent fluctuations as it has for the other three configurational setups too. This is again likely due to irradiance scattering onto the thermocouple or interferences from the wind.

For the same run a graph of T outlet actual versus T outlet theoretical is shown in Figure 4-9. The Figure gives the temperature against the time of day. For both data sets trend lines were

added. The results show that the outlet temperature could be about 20 °C warmer if losses were minimised or eliminated. Unusually the trend line for both data sets slants downwards. This may be caused by partial cloud cover interfering and scattering the sunlight. This is backed up by the radiometric data, since the DNI sharply decreased toward the end of the run, and as such the GHI decreased too.

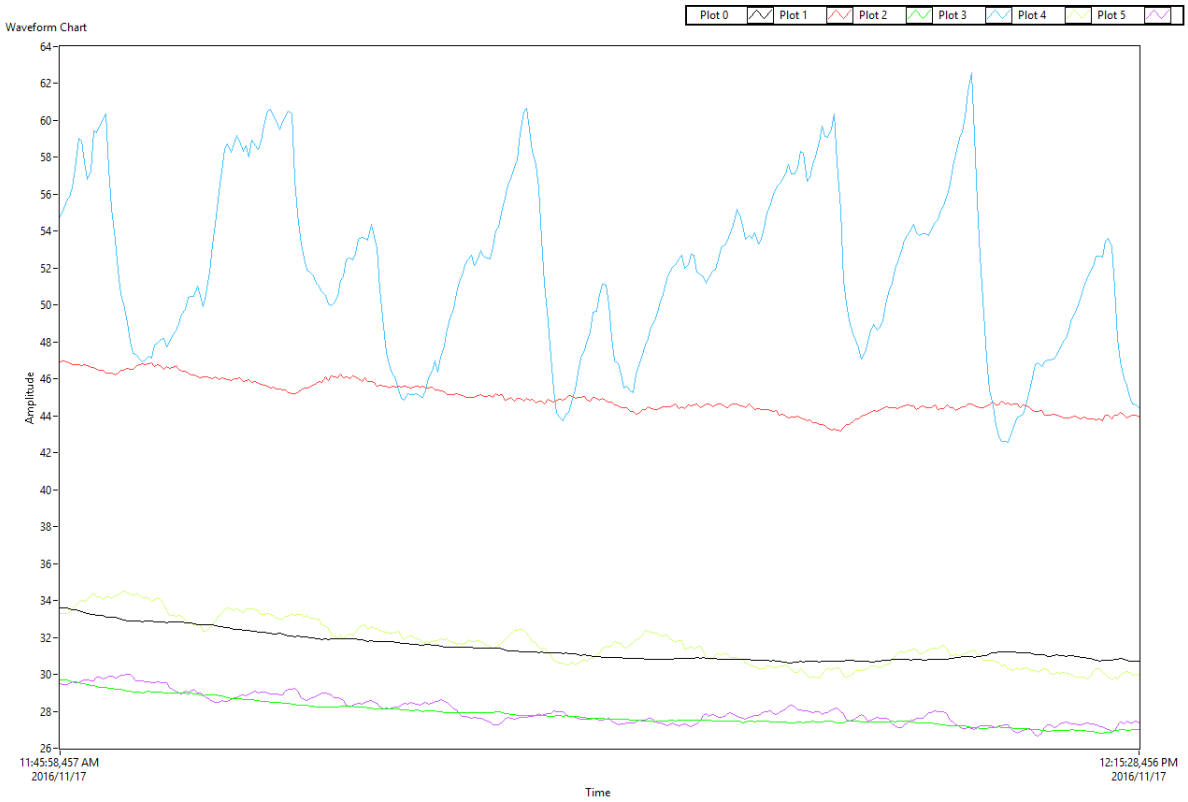

Figure 4-8: Raw data of the experiment conducted on the 17th of November exported from LabVIEW™

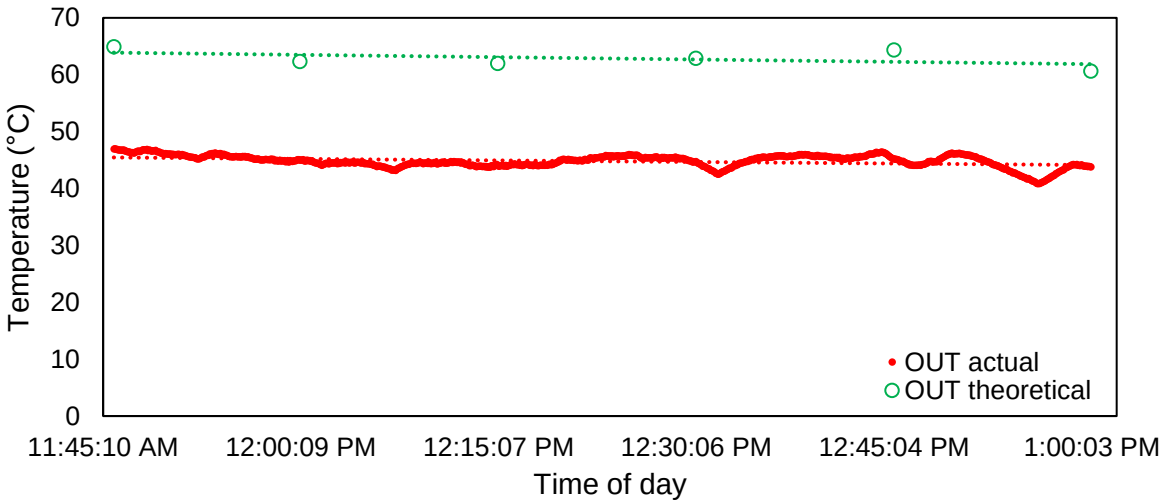

Figure 4-9: Temperature vs time of day graph of the actual outlet temperature and the theoretical outlet temperature for the configuration painted receiver, glass mirror strips

A comparison of the eight runs recorded for the arrangement is given in Table 4-5. The results are all fairly similar which shows good repeatability. The data is also very stable as the difference between average ΔT and the maximum ΔT rarely exceeds 2 °C. The one property that did fluctuate significantly was the surface temperature of the pipe, which was expected from previous results. The standard deviation of the receiver temperature in any given run was significantly higher than any other measurement. This shows that its data is unreliable to a certain extent, which needs to be taken into consideration when drawing conclusions. For standard deviation data consult Appendix 2. The temperature of the mirrors was low and comparable to the ambient temperature of the run. In each run a significant amount of energy was transferred to the water as $\dot{Q}_{actual}$ in each case was more than 1000 W. Despite this the calculated efficiencies were still low ranging between 40 % and 52 %. On average the efficiency for this configuration was 45 % and as expected the highest energy transferred was achieved.

Table 4-5: Data averaged for all runs using glass mirrors and a painted receiver

Date	**2016/10/31**		**2016/11/04**			**2016/11/17**		
Time	11:45-13:00	13:00-14:15	10:30-11:45	11:45-13:00	13:00-14:15	10:30-11:45	11:45-13:00	13:00-14:15
Avg ΔT (°C)	13.01	12.18	11.63	15.38	13.86	12.21	12.90	11.52
Max ΔT (°C)	15.18	13.82	13.12	16.62	15.80	14.64	14.34	12.83
Avg T_{AMB} (°C)	34.33	35.98	28.10	30.22	30.94	27.91	28.26	30.87
Avg T_s (°C)	71.33	57.51	47.07	53.91	62.74	51.26	52.36	53.72
Avg T_{CONC} (°C)	37.78	37.82	32.46	34.09	33.62	33.20	31.09	31.56
T_{TANK} start (°C)	33.22	37.37	29.21	28.98	30.16	26.71	29.72	29.42
T_{TANK} end (°C)	37.35	37.83	28.90	30.06	33.94	29.71	29.44	31.97
$\dot{Q}_{actual}$ (W)	1196.3	1120.3	1069.0	1413.9	1274.2	1122.9	1185.8	1065.9
Avg GHI (W/m^2)	1039.8	936.3	978.5	1030.0	946.7	1066.9	1076.8	981.9
$\dot{Q}_{theo}$ (W)	2715	2445	2555	2670	2472	2786	2812	2564
η (%)	44.1	45.8	41.8	52.6	51.5	40.3	42.2	41.7

Chapter 5: Comparison and Discussion

This chapter serves to compare both observations and logged data of the possible arrangements. At the end of the chapter a comparison to an industrial standard LFC module is made. Conclusions drawn from this chapter and the preceding chapter are reported in the next chapter.

5.1 Unpainted Pipe vs. Painted Pipe

The first experiments were conducted on the unpainted receiver which had a faded black colour. After sufficient data was gathered the pipe was painted with two coats of a semi matte black paint. In order to better visualise the difference of the two a photograph of the pipe being painted is show in Figure 5-1. The unpainted pipe is on the left of the Figure, while the newly painted pipe is on the right. As can be seen in the Figure the initial condition of the pipe is a faded black with a lot scratches revealing the metal underneath. In comparison the newly painted section looks much more homogenous and has a crisp, strong black colour. The paint was relatively inexpensive and cost R 200 for 1 L. The properties that are expected to be affected after painting the receiver are: the surface temperature of the pipe, the outlet temperature of the pipe and therefore the ΔT, the energy supplied to the water and the efficiency of the setup. In all cases an increase was expected.

Figure 5-1: Photograph of the unpainted pipe (left) and the semi-matte black painted pipe (right)

For a simpler overview the runs with the concentrator stainless steel sheet will be compared first, followed by the runs using the mirrors. A comparison of the two assemblies using the metal sheet is given in Table 5-1. For comparative purposes the averages of the values reported in the previous chapter are shown. From the table it can be seen that the surface temperature of the pipe did not increase significantly as was expected. However, the water in the pipe gained more energy after the pipe had been painted. This shows that there was a small benefit to painting the pipe. Overall the efficiency, given in percentage, decreased after painting the pipe. This is likely due to the constants used in calculating the theoretically attainable energy. It is possible that the unpainted pipe actually has a higher absorptivity value or the painted pipe has a lower absorptivity value. Even though the surface temperature of the receiver did not show an increase, the effect of painting the pipe can clearly be seen in the temperature difference of the water.

Table 5-1: Comparison of an unpainted and painted pipe when using stainless steel sheet metal

Property	Unpainted	Painted
T_s (°C)	43.3	43.1
ΔT (°C)	2.8	3.6
$\dot{Q}_{actual}$ (W)	258	332
η (%)	14	13

In this case the average surface temperature of the receiver hardly changed after painting it. This is especially true when considering the tolerance limits of the thermocouples. However, this may also be an error in measurement, since the water was heated more on average. This should only make sense if more energy was supplied to the receiver, resulting in a higher surface temperature. As mentioned in the previous chapter the reading was highly unstable and had the highest standard deviation value. Errors in measurement could likely be due to sunlight scattering striking the thermocouple. Another factor that was previously not mentioned is the influence the wind had. The testing field provided no natural barriers against wind and was often subjected to strong gusts. As metal conducts heat very well, it is possible wind would cause the receiver's temperature to drop sharply, while the temperature of the water would only be affected to a lesser extent. Comparison of the other properties shows that the painted pipe allowed more heat to be supplied to the water in it. As with the sheets the efficiency lowered which brings into question the validity of the values chosen as absorptivity constants. The same table for runs with the glass mirror strips is constructed in Table 5-2.

Table 5-2: Comparison of the data for an unpainted and painted receiver with glass mirrors as the concentrator

Property	Unpainted	Painted
T_s (°C)	59.5	56.2
ΔT (°C)	11.4	12.8
$\dot{Q}_{actual}$ (W)	1049	1181
η (%)	54	45

5.2 Stainless Steel Sheet Metal vs. Glass Mirror Strips

The cost of the stainless steel metal sheets, as well as the 200 mirror strips, was approximately R 3000. This cost does not include any costs incurred from maintenance or buying additional equipment to maintain the type of concentrator. 200 strips are glass mirror were bought so that spares were available if something should happen to the strips. Since the cost for both types of concentrator was the same, a comparison of the two is made much easier. It allows the focus to be on the effectiveness of the concentrator. However, there are other characteristics that need to mentioned and compared.

The density of stainless steel 304 is 7861 kg/m^3. The sheet metal used was 1.5 mm thick and this enables the mass of sheets to be calculated. This weight of 61.3 kg had to be supported by the metal frame of the rig. In comparison, glass has a density of 2500 kg/m^3 and the weight of the combined strips present on the rig during testing was 40.8 kg. The difference is quite significant as the metal is 1.5 times as heavy as the glass strips. This shows that the metal sheets subjected the rig to a higher load which might have a serious impact over a prolonged time period.

Another important consideration is the load caused by wind. Since the glass mirror is discretised into individual strips, there is very little wind resistance when using this concentrator. The wind can simply pass through in the area between the mirror segments. A photograph of the strips of glass mirror is given in Figure 5-2. Highlighted in red in the Figure is the receiver and the incident sunlight on it.

Figure 5-2: Photograph of the glass mirror strips reflecting light onto the receiver (highlighted in red)

In contrast to the mirrors, the sheet metal has a broad area that provides resistance to any wind. The effect of this was observed during experimentation, as strong blows would subject the rig to visible load. Fortunately the assembly could handle the load and no problems were encountered. The same cannot be said for the glass mirrors. During testing a strong gust caused some of the mirror strips to oscillate violently, which resulted in 21 strips snapping. The broken strips had to be replaced and it proved how fragile the glass mirror strips are. A photograph of the broken mirror strips can be seen in Figure 5-3.

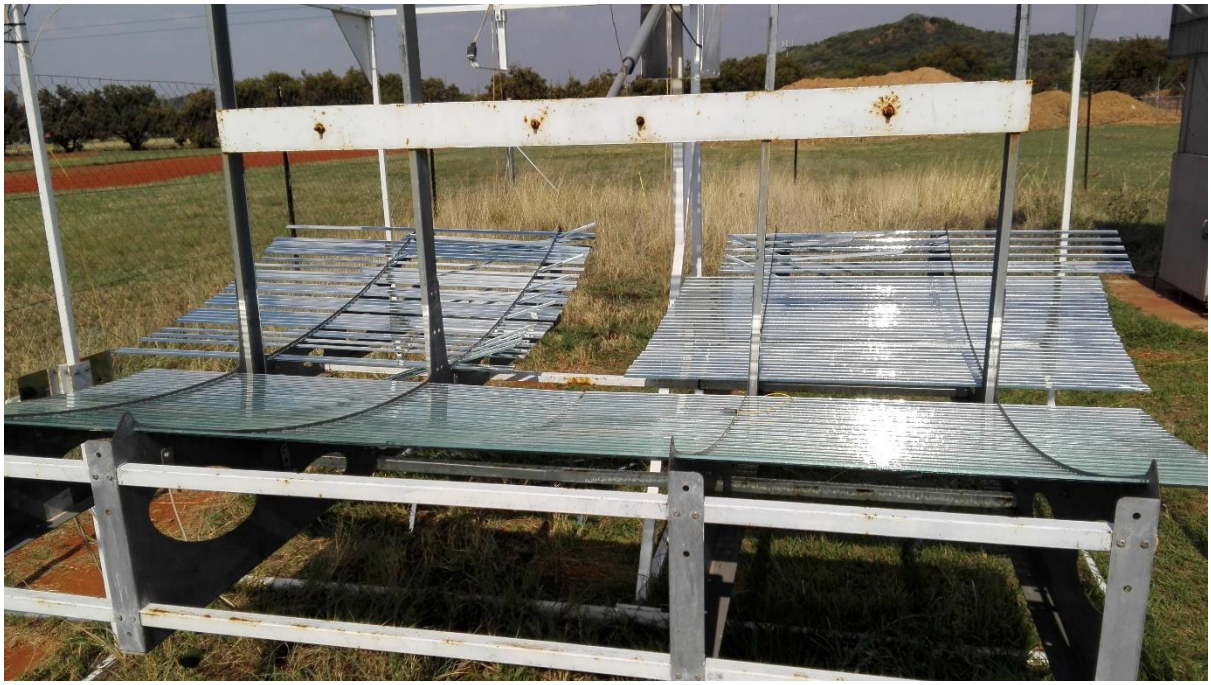

Figure 5-3: Photograph taken of the rig after 21 mirror strips snapped due to wind

While precautions were taken in future runs to prevent the same from happening, it is important to consider the effects weather can have. For instance, while both types of concentrator were left outside overnight, the metal sheets were noticeably dirtier the next day. The sheets had pockets where water collected and dirt would deposit. The mirrors were also noticeably dirty, especially after rain, but there were no obvious patches where dirt gathered. The mirrors were also easier to clean before starting a run. Fortunately neither concentrator had to survive a hail storm, but it is hypothesised that the metal would fare better. The destructive power of hail would surely mean that both concentrators would suffer, but it is likely the glass mirrors would be completely destroyed. This hypothesis is preferably not tested due to economic constraints. Most of the spare mirror strips were used because of the wind incident.

Another consideration is the maintenance of the type of concentrator. Since the strips of glass mirror were proven to be fragile, it is not unreasonable to assume they will incur a higher maintenance cost. However, by separating the glass mirror into individual strips, it is possible to replace only the damaged strips. Nevertheless a tarp or some other form of protection

should be considered to ensure the prevention of any potential damage to the glass mirrors. This is especially true if the mirrors are left outside for prolonged periods of time or during stormy weather. Stainless steel metal is expected to tolerate stormy weather better than glass mirrors. If it is not looked after properly it can weather and rust. In this case the entire piece of sheet metal would have to be replaced which would incur great costs. As such it advisable to consider protecting the sheet metal when the rig is not in use. It is difficult to conclusively tell which concentrator type would ultimately have the lower maintenance cost. Ultimately the location of the setup and its typical weather conditions will affect which type of concentrator will be the most economically viable.

Before considering the effectiveness of each type of concentrator, it is worth discussing how well the type of concentrator focuses light onto the receiver. It was noticed that the arc followed by the stainless steel sheet metal was not the same for the glass mirrors. It was also observed that the metal sheets had a secondary focal point, which was confirmed by moving the rig so that this focal point hit the pipe. Comparing the two, it was clear to see that the secondary focal point was far less intense than the primary focal point and likely due to dents or imperfections in the metal. The mirrors had the benefit of allowing each strip to be angled in such a way that each focuses onto the same focal point. In order to compare and potentially substantiate these findings the surface temperature of the receiver for each configuration is plotted in Figure 5-4. It is argued that a good focal point would mean less irradiance interference on the thermocouple measuring the surface temperature of the receiver. This would in turn mean a more stable pipe temperature reading. The data, however, is erratic and difficult to make sense of. Therefore major horizontal axis gridlines are constructed and trend lines for the four data sets are added. These are compared to determine the more stable receiver temperature.

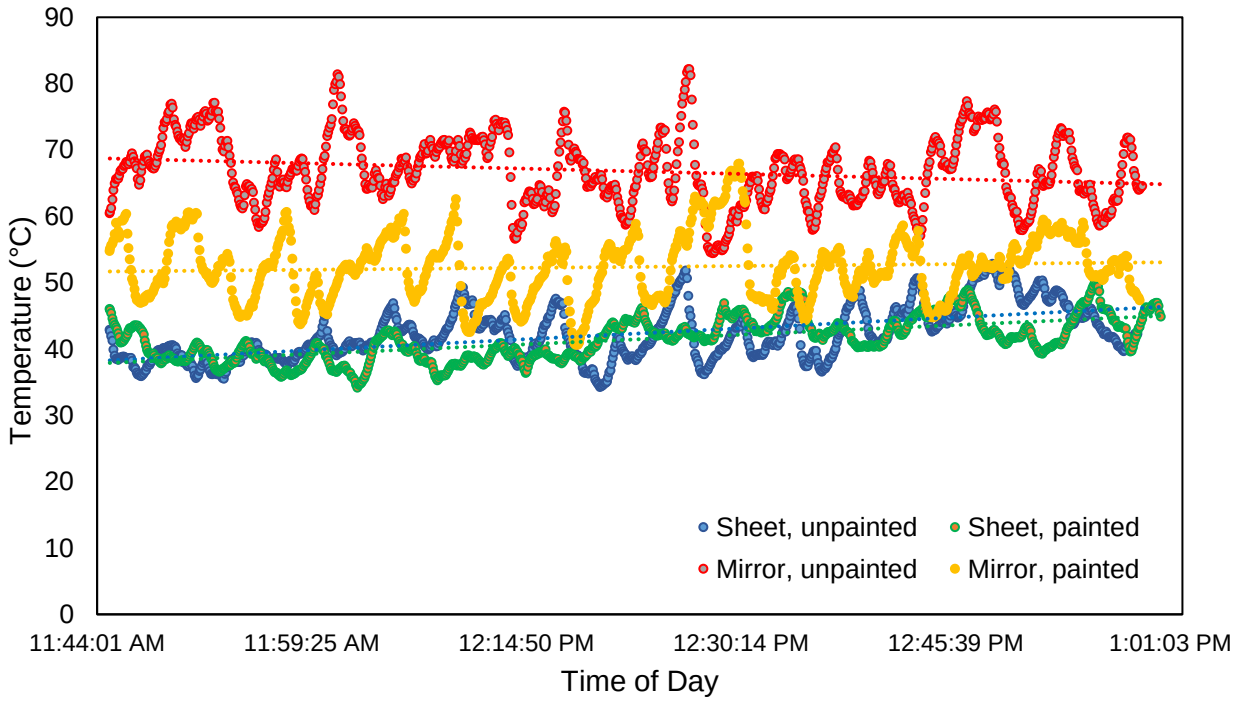

Figure 5-4: Surface temperature of the pipe for the four different configurations

At first glance it looks as if the data for the glass mirrors is more erratic. However, after fitting a linear trend line it is revealed that the sheet metal data is more variable. This can be seen by the slope of the trend line. For the configuration metal sheet and unpainted receiver, the trend line starts at 39 °C and climbs to 47 °C. After the receiver had been painted the configuration showed a similar trend, starting at the same point and ending at 46 °C.

In contrast the assembly with mirror strips and a painted pipe had an almost constant receiver temperature that only increased slightly over the course of then run. The run with mirror strips and an unpainted receiver shows more variable trend line, starting at 69 °C and ending at 65 °C. This shows that while the mirrors are more stable and focus sunlight better than the sheet metal, they can also have inaccuracies.

Now that the concentrators are better understood, their effectiveness at heating up water by reflecting sunlight onto a single focal area in a PTC setup can be compared. The measured properties the concentrator affects are much the same as those already mentioned in this chapter. In order to compare the two types of concentrator these averaged values are given again in Table 5-3. In addition to the reiterated values is the temperature value of the concentrator. In this instance the receiver had been unpainted.

Table 5-3: Comparison of sheet metal versus glass mirrors for an unpainted pipe

Property	Stainless Steel Sheet	Glass Mirror Strips
T_s (°C)	43.3	59.5
T_{CONC} (°C)	43.9	32.8
ΔT (°C)	2.8	11.4
$\dot{Q}_{actual}$ (W)	258	1049
η (%)	14	54

The data is telling in how stark the difference between the sheet metal and the glass mirrors is. Not only was the temperature of the concentrator 11 °C lower for the glass mirror setup, but the efficiency and energy supplied were almost four times that of the setup using stainless steel as a concentrator. This truly shows how much more effective using glass mirrors was. The same findings are given in Table 5-4, in which both concentrators when using a painted receiver are compared.

Table 5-4: Comparison of sheet metal versus glass mirrors for a painted pipe

Property	Stainless Steel Sheet	Glass Mirror Strips
T_s (°C)	43.1	56.2
T_{CONC} (°C)	47.0	34.0
ΔT (°C)	3.6	12.8
$\dot{Q}_{actual}$ (W)	332	1181
η (%)	13	45

These two tables substantiate the findings of the chapter. Discretised mirror strips are far better at concentrating light in a PTC setup than stainless steel sheet metal. They are also more economically viable and have a number of advantages over using a large, single, curved mirror, such as lighter mass, smaller wind load and strips can be replaced individually if damaged.

5.3 Comparison of Glass Mirror Strips to Industrial Standard LFC

The industrial standard that was compared to the setup in question was taken from a data sheet found on Industrial Solar's website. The technical data sheet details the module LF-11 and lists its expected specifications, as well as operating conditions. While the setup used was not an LFC, by using discretised glass mirror strips as a concentrator, there are a lot of similarities and it is therefore compared to one. The most notable difference between the rig and an LFC is that the mirrors are not individually moved to track the sun, but instead are fixed and the entire metal frame is moved. Other notable differences include the size of the module, the size of the mirrors used, the type of THF used and the use of a vacuum absorber. To summarise these differences, as well as compare the outputs of the different configurations, Table 5-5 is constructed.

Table 5-5: Comparison of the tested PTC with glass mirrors as the concentrator and an industrial standard LFC module, LF-11

Property	Rig with glass mirror strips	LF-11
Solar tracking	Very basic, frame follows the sun	Advanced, each mirror tracks the sun individually
Module width (m)	2.3	7.5
Module length (m)	2.5	4.06
Surface area of reflectors (m)	4.08	22
Vacuum absorber	No	Yes
Peak thermal output based on reflector area (W/m^2)	346.5	562
Thermal output based on total installation area (W/m^2)	117.8	375

The table indicates that the rig is inferior in every aspect, but it must be made clear that LF-11 has been optimised so that its aperture size is as small as it can be, as well as optimal solar tracking. Its heat losses have also been minimised by using a vacuum absorber. While both modules possess secondary reflectors to focus scattered sunlight, the rig's secondary reflectors consist of metal which, unlike the glass mirror used for LF-11, is not very reflective. It is known that the rig has many shortcomings and areas that can be improved upon, but for all its short comings, it fares quite well. Its peak thermal output is approximately 62 % of the LFC's peak thermal output. Besides the peak thermal output for the LF-11 module is only achieved when stringent conditions are met:

- ambient temperature is 30 °C
- inflow temperature of 160 °C
- outflow temperature of 180 °C
- 900 W/m^2 direct normal radiation

For this reason the results from the parabolic collector using strips of glass mirror as a concentrator are comparable to an industrial type LFC. However, there are still significant improvements that can be undertaken to achieve better results.

A telling property is the large discrepancy of the thermal output based on the installation area. In this aspect the PTC tested achieves only 31 % of the presented LFC value. This is mostly due to the manner in which the rig is set up. LFCs are advantageous over PTCs since they require a smaller installation area to achieve the same output. Since the tested rig is really a PTC with an LFC type concentrator it does not have this advantage. Instead it takes up a much larger installation area, like a PTC would, which is evident from the thermal output value based on installation area. Using discretised mirror strips does, however, share many advantages with an LFC, such as: lower manufacturing cost, lower wind loads and lighter concentrator mass meaning less load on the support structure. By combining LFC technology with a standard parabolic trough design and using thin glass mirror strips as a concentrator, a novel design of a PTC has been achieved. The design is very basic and has many properties that can be improved, such as use of a vacuum absorber, better solar tracking and optimising aperture size. The rig was successfully characterised and can be used on its own as is to heat water. It could also prove to be viable at industrial scale and more research into this field is required.

Chapter 6: Conclusions and Recommendations

The parabolic trough collector was successfully characterised, but the theoretical model is very basic and does not adequately consider losses. To improve this, it recommended that simulations on the PTC are carried out and a better model built. The PTC did successfully heat up water beyond the standard limits of tolerance values attributed to K type thermocouples. Losses to the environment were still significant and could be limited or omitted with the installation of a glass vacuum absorber. They could also be better understood if convective losses are modelled and wind measurements are taken on site. This is recommended for future tests. Two different types of concentrator were successfully implemented and were compared.

The stainless steel had an average efficiency of 14 % when the receiver was unpainted and 13 % when the receiver was painted. The glass mirror strips had average efficiencies of 54 % and 45 % for an unpainted and painted receiver respectively. While these values are not a true representation of the efficiency of the overall setup, they do enable the different setups to be compared. This can be improved upon if a better model exists. A more telling property is the actual amount of energy supplied to the thermal heating fluid. For this the averaged values over all the experimental runs conducted for stainless steel sheet metal were 258 W and 332 W for an unpainted and painted pipe respectively. When using the glass mirrors an average energy value of 1049 W was supplied when the pipe was unpainted and an average of 1181 W was gained in the runs conducted after the pipe had been painted.

Painting the receiver had little to no effect. The surface temperature of the receiver after painting the pipe was not higher and a slight increase in the energy gained by water was observed. This can be explained by inaccuracies during testing and it is recommended that these tests are carried out again. The tests should be designed in such a way to completely omit irradiance affecting the thermocouple taking the measurement. The difference in energy gain after painting the pipe indicates that the absorptivity of the pipe initially was already high. It also shows that energy is lost elsewhere and the absorptivity of the pipe was not in this case a significantly limiting factor. A suggestion to improve the effectiveness of the PTC is to insulate the receiver in a vacuum by using a glass shield, as this would lower losses to the environment. It is, however, recommended that other paints be considered for future testing.

Great care needs to be taken of the concentrator in a parabolic trough collector design. This is especially true for the glass mirror strips which were shown to be fragile. In windy conditions caution needs to be exercised to avoid mirror strips from oscillating, as this can lead to them snapping. It is recommended that they are protected by means of a tarp when they are not being used.

Strips of glass mirror are not only viable but fared far better than its metal sheet counterpart. On average the glass mirrors supplied almost four times the heat the metal sheets supplied. Glass mirrors also had a more stable receiver surface temperature measurement and concentrated light onto a focal point more accurately than the metal sheets. An observation was noted of the stainless steel metal sheet having more than one focal point which means sunlight was not being accurately concentrated. During experimental runs the temperature of glass mirror concentrator was a significant 11 °C lower than the temperature of the metal sheets. This explains to some extent why the mirrors outperformed the sheet metal.

Using thin glass mirror strips as a concentrator successfully applied LFC technology to a parabolic trough design, resulting in a novel type of PTC. It is recommended that mirror strips be used as a concentrator for future runs and be considered for industrial scale. Compared to an industrial module LF-11, the peak thermal output achieved was 346 W/m^2, whereas the industrial value given was 562 W/m^2. While the discrepancy was large, the differences in design of the compared modules were also significant. It is therefore believed that results are comparable, as better thermal outputs are expected to be achieved after addressing the inherent flaws in the design of the tested PTC. The mirror strips shared many advantages with an LFC design, since they are much less expensive to manufacture than a curved mirror. They provide little to no wind resistance due to the aperture distance between strips. The strips can also be replaced individually if the need arises. The design does have the drawback that it requires a large installation area, similar to power plants using PTC technology. It is recommended that more research and emphasis is put into this field as an alternative energy power plant for South Africa.

Chapter 7: References

This chapter gives all references used in this dissertation in alphabetical order. References were given when work or information from other sources was cited.

Alguacil, M, Prieto, C, Rodriguez, A and Lohr, J (2014) “Direct Steam Generation in Parabolic Trough Collectors” *Energy Procedia*, 49, 21 - 29.

Barriga, J, Ruiz-de-Gopegui, U, Goikoetxea, J, Coto, B and Cachafeiro, H (2014) “Selective Coatings for New Concepts of Parabolic Trough Collectors” *Energy Procedia,* 49, 30 - 39.

Brooks, MJ (2005) “Performance of a Parabolic Trough Solar Collector” Master’s Thesis, University of Stellenbosch, SA.

Brooks, MJ, du Clou, S, van Niekerk, JL, Leonard, C, Mouzouris, MJ, Meyer, AJ, van der Westhuizen, N, van Dyk, EE and Vorster, F (2015) “SAURAN: A new resource for solar radiometric data in Southern Africa” *Journal of Energy in Southern Africa*, 26, 2-10.

Brooks, MJ, Mills, I and Harms, TM (2006) “Performance of a Parabolic Trough Collector” *Journal of Energy in Southern Africa*, Vol 17, No 3.

Çengel, YA and Ghajar, AJ (2011) *Heat and Mass Transfer*, 4th ed, McGraw-Hill, New York.

Conibeer, G (2007) “Third-generation Photovoltaics” *Materials Today*, Vol 10, No 11.

Dekker, J, Nthontho, M, Chowdhury, S and Chowdhury, SP (2012) “Investigating the Effects of Solar Modelling Using Different Solar Irradiation Data Sets and Sources within South Africa” *Solar Energy*, 86, 2354 - 2365.

Fluri, TP (2009) “The Potential of Concentrating Solar Power in South Africa” *Energy Policy*, 37, 5075 - 5080.

Garcia, ET, Ogueta-Gutierrez, M, Avila, S, Franchini, S, Herrera, E and Meseguer, J (2014) “On the Effects of Windbreaks on the Aerodynamic Loads over Parabolic Solar Troughs” *Applied Energy*, 115, 293 - 300.

Government Gazette (2010) “Air Quality Act, 2004 (Act no 34 of 2004)” No33064, *Vol 537*, 31 March 2010.

Hachicha, AA, Rodriguez, I, and Oliva, A (2014) “Wind Speed Effect on the Flow Field and Heat Transfer around a Parabolic Trough Solar Collector” *Applied Energy*, 130, 200 - 211.

Industrial Development Corporation (2012) “Green Economy Report: The cost evolution of renewable energies” *Department of Research and Information*, Sandton, SA.

Industrial Solar (*sa*) “Technical Data Industrial Solar linear Fresnel collector LF-11” http://www.industrial-solar.de/content/produkte/fresnel-kollektor/ [2017, January 19].

IRENA (2012) “Concentrating Solar Power” Renewable Energy Technologies: Cost Analysis Series, Vol 1: Power Sector, Bonn, Germany.

Kumar, KR and Reddy, KS (2012) “Effect of Porous Disc Receiver Configurations on Performance of Solar Parabolic Trough Concentrator” *Heat Mass Transfer*, 48, 555 - 571.

Meiser, S, Lüpfert, E, Schiricke, B and Pitz-Paal, R (2014) “Analysis of Parabolic Trough Concentrator Mirror Shape Accuracy in Different Measurement Setups” *Energy Procedia*, 49, 2135 - 2144.

Meyers, RA (2012) *Encyclopedia of Sustainability Science and Technology*, Springer, New York.

Miqdam Tariq, C Khalil IA, Hussein A Kazem, Feras Hasoon, Hakim S Sultan Aljibori, Ali AK Alwaeli, Firas S Raheem and Ali HAAlwaeli (2012) “Effect of Design Variation on Saved Energy of Concentrating Solar Power Prototype” *Proceedings of the World Congress on Engineering,* Vol III, WCE 2012.

Morin, G, Dersch, J, Platzer, W, Eck, M and Häberle A (2012) “Comparison of Linear Fresnel and Parabolic Trough Collector power plants” *Solar Energy*, 86, 1-12.

National Instruments Corporation (2009) “NI USB-9213 User Guide and Specifications”.

OMEGA (*sa*) "ANSI and IEC Color Codes for Thermocouples, Wires and Connectors" http://www.omega.com/techref/colorcodes.html [2017, March 1].

Österholm, R and Pålsson, J (2014) "Dynamic Modelling of a Parabolic Trough Solar Power Plant" *Proceedings of the 10th International Modelica Conference.*

Pitz-Paal, R (2012) "Parabolic Trough, Linear Fresnel, Power Tower: A Technology Comparison" www.iass-potsdam.de/sites/default/files/files/12.5-iass_pitz-paal.pdf [2017, January 19].

REN21 (2016) *Renewables 2016 Global Status Report*, Paris: REN21 Secretariat.

Ruegamer, T, Kamp, H, Kuckelkorn, T, Schiel, W, Weinrebe, G, Nava, P, Riffelmann, K and Richert, T (2014) "Molten Salt for Parabolic Trough Applications: System Simulation and Scale Effects" *Energy Procedia*, 49, 1523 - 1532.

Russell, R (2010) "Solar Radiation at Earth" *Windows to the Universe*, http://www.windows2universe.org/earth/climate/sun_radiation_at_earth.html [2014, August 1].

Sawin, JL and Martinot, E (2011) "Renewables Bounced Back in 2010, Finds REN21 Global Report", http://www.renewableenergyworld.com/rea/news/article/2011/09/renewables-bounced-back-in-2010-finds-ren21-global-report [2014, June 26].

Solar Energy Research Institute (1985) *Silver/Glass Mirrors for Solar Thermal Systems*, U.S. Governmental Printing Office, Washington.

Solar Millenium AG (*sa*), "Description of a solar thermal plant with thermal storage", http://www.solarmillennium.de/english/downloads/index.html [2017, January 19].

Wang, Y (2008) "Chasing the Sun Concentrated Solar Power" https://www.mtholyoke.edu/~wang30y/csp/PTPP.html [2017, January 19].

World Meteorological Organisation (2016) "WMO Greenhouse Gas Bulletin" *The State of Greenhouse Gases in the Atmosphere Based on Global Observations*, No 12.

Wilson, G and Emery, K (2014) “Conversion Efficiencies of Best Research Solar Cells Worldwide from 1976 to 2014 for Various Photovoltaic Technologies” *National Renewable Energy Laboratory*, Golden Co.

Winkler, H (2005) “Renewable Energy Policy in South Africa: Policy Options for Renewable Electricity” *Energy Policy*, 33, 27 – 38.

Xie, XT, Dai, YJ, Wang, RZ and Sumathy, K (2011) “Concentrated solar energy applications using Fresnel lenses: A review” *Renewable and Sustainable Energy Reviews*, 15, 2588-2606.

Xu, L, Wang, Z, Li, X, Yuan, G, Sun, F, Lei, D and Li, S (2014) “A Comparison of Three Test Methods for Determining the Thermal Performance of Parabolic Trough Solar Collectors” *Solar Energy*, 99, 11 - 27.

Appendix 1

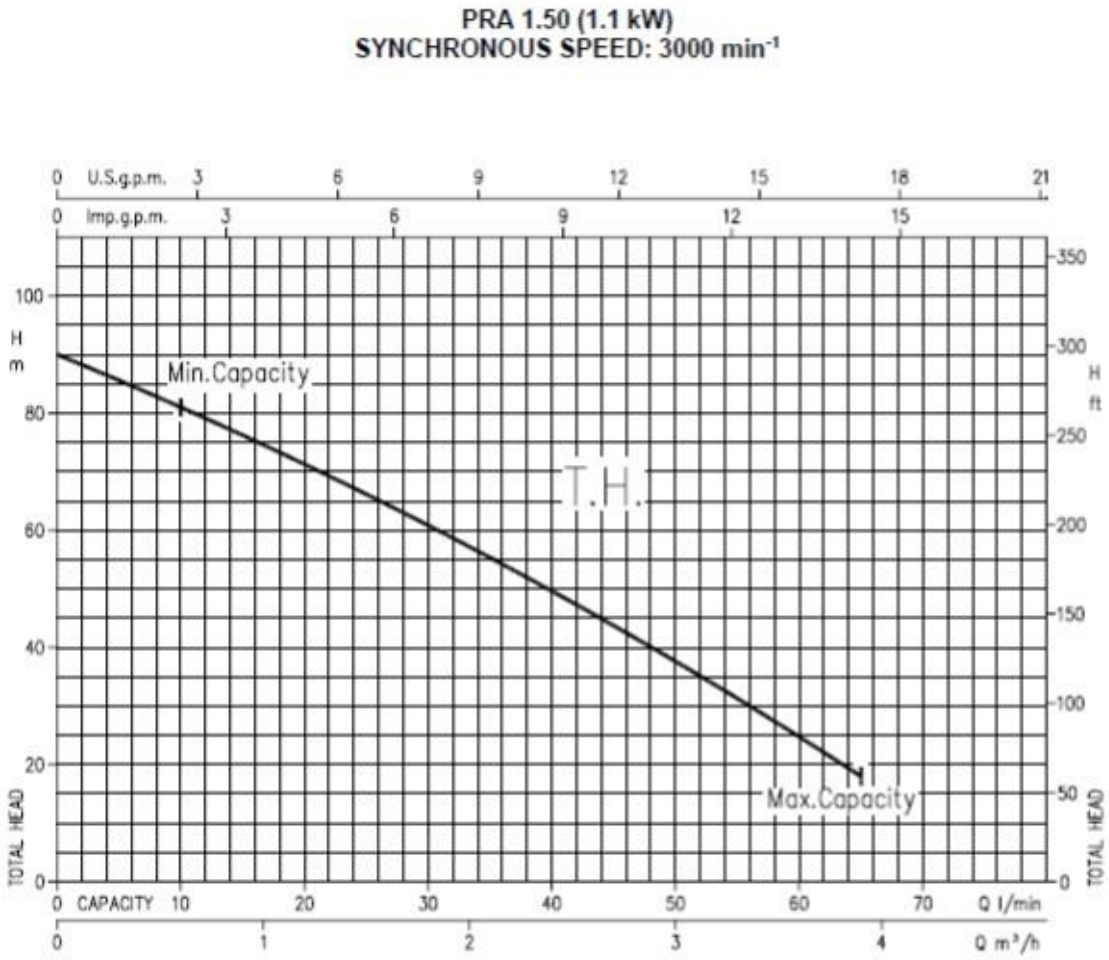

Figure A-1: Pump curve for an Ebara PRA 1.50 pump

Appendix 2

Table A- 1: Standard deviation values for metal sheets, unpainted pipe

Date	2016/10/11			2016/10/12			2016/10/25		
Time	10:30-11:45	11:45-13:00	13:00-14:15	10:30-11:45	11:45-13:00	13:00-14:15	10:30-11:45	11:45-13:00	13:00-14:15
std dev IN	1.64	0.91	0.40	0.33	1.32	0.47	0.85	0.87	0.59
std dev OUT	1.67	0.93	0.88	0.68	1.36	0.70	0.92	1.07	0.88
std dev TANK	0.18	0.91	0.57	0.14	1.26	0.47	0.89	0.76	056
std dev REC	5.40	3.41	2.94	3.29	3.09	2.36	1.93	2.87	1.84
std dev CONC	2.01	1.83	1.34	2.07	3.17	1.79	0.95	2.12	1.49
std dev AMB	0.48	1.11	0.74	0.46	0.97	0.67	0.84	0.92	0.80

Table A- 2: Standard deviation values for mirror strips, unpainted pipe

Date	2016/10/26			2016/10/27			2016/10/28	
Time	10:30-11:45	11:45-13:00	13:00-14:15	10:30-11:45	11:45-13:00	13:00-14:15	10:30-11:45	11:45-13:00
std dev IN	2.00	0.71	0.25	0.55	0.71	0.44	0.46	0.24
std dev OUT	2.27	1.50	1.02	1.28	1.10	0.93	0.97	0.62
std dev TANK	0.46	0.64	0.09	0.58	0.61	0.43	0.35	0.13
std dev REC	4.81	5.34	4.06	5.60	5.11	5.31	5.50	3.55
std dev CONC	1.23	0.87	0.67	0.73	1.18	1.04	0.71	0.51
std dev AMB	0.51	0.74	0.49	0.68	0.70	0.59	0.31	0.39

Table A- 3: Standard deviation values for metal sheets, painted pipe

Date	2016/11/18			2016/11/28			2016/11/30		
Time	10:30-11:45	11:45-13:00	13:00-14:15	10:30-11:45	11:45-13:00	13:00-14:15	10:30-11:45	11:45-13:00	13:00-14:15
std dev IN	0.09	0.72	1.32	0.14	0.84	0.86	1.10	0.50	0.32
std dev OUT	0.40	1.00	1.20	0.38	0.75	1.25	1.02	0.70	0.63
std dev TANK	0.09	0.71	0.64	0.08	0.78	0.67	0.96	0.36	0.36
std dev REC	1.06	2.88	2.96	2.36	2.52	3.12	1.97	1.92	1.85
std dev CONC	1.10	2.01	2.28	1.16	1.76	2.40	1.84	1.60	1.52
std dev AMB	0.16	0.73	0.79	0.36	0.89	0.60	1.00	0.35	0.46

Table A- 4: Standard deviation values for mirror strips, painted pipe

Date	2016/11/31		2016/11/04			2016/11/17		
Time	11:45-13:00	13:00-14:15	10:30-11:45	11:45-13:00	13:00-14:15	10:30-11:45	11:45-13:00	13:00-14:15
std dev IN	0.71	0.58	0.63	1.24	0.38	0.79	0.74	0.51
std dev OUT	1.18	1.14	1.40	1.85	1.11	1.67	1.02	0.98
std dev TANK	0.58	0.55	0.47	0.37	0.29	0.68	0.68	0.42
std dev REC	6.49	4.50	6.36	4.70	6.24	6.82	4.94	4.41
std dev CONC	1.06	0.87	0.88	0.61	0.83	0.87	0.92	0.57
std dev AMB	0.54	0.74	0.38	0.53	0.54	0.81	0.78	0.60